

## THE SIZES AND LUMINOSITIES OF MASSIVE STAR CLUSTERS

NORMAN MURRAY<sup>1,2</sup>*Draft version November 6, 2018*

## ABSTRACT

The masses of star clusters range over seven decades, from ten up to one hundred million solar masses. Remarkably, clusters with masses in the range  $10^4 M_\odot$  to  $10^6 M_\odot$  show no systematic variation of radius with mass. However, recent observations have shown that clusters with  $M_{cl} \gtrsim 3 \times 10^6 M_\odot$  do show an increase in size with increasing mass. We point out that clusters with  $M_{cl} \gtrsim 10^6 M_\odot$  were optically thick to far infrared radiation when they formed, and explore the hypothesis that the size of clusters with  $M_{cl} \gtrsim 3 \times 10^6 M_\odot$  is set by a balance between accretion powered radiation pressure and gravity when the clusters formed, yielding a mass-radius relation  $r_{cl} \sim 0.3(M_{cl}/10^6 M_\odot)^{3/5}$  pc. We show that the Jeans mass in optically thick objects increases systematically with cluster mass. We argue, by assuming that the break in the stellar initial mass function is set by the Jeans mass, that optically thick clusters are born with top heavy initial mass functions; it follows that they are over-luminous compared to optically thin clusters when young, and have a higher mass to light ratio  $\Upsilon_V = M_{cl}/L_V$  when older than  $\sim 1$  Gyr. Old, optically thick clusters have  $\Upsilon_V \sim M_{cl}^{0.1-0.3}$ . It follows that  $L_V \sim \sigma^\beta$ , where  $\sigma$  is the cluster velocity dispersion, and  $3.6 \lesssim \beta \lesssim 4.5$ . It appears that  $\Upsilon_V$  is an increasing function of cluster mass for compact clusters and ultra-compact dwarf galaxies. We show that this is unlikely to be due to the presence of non-baryonic dark matter, by comparing clusters to Milky Way satellite galaxies, which are dark matter dominated. The satellite galaxies appear to have a fixed mass inside a fiducial radius,  $M(r=r_0) = const..$

*Subject headings:* galaxies: star clusters — stars: mass function

## 1. INTRODUCTION

Most stars in the Milky Way are believed to have formed in star clusters, e.g., Lada & Lada (1995). In their review Clarke et al. (2000) note that 96% of stars in the Orion B cloud are in clusters, while 50–80% of stars in Orion A are. The latter fraction is consistent with that found by Gomez et al. (1993) in Tarus. Allen et al. (2007) suggest that only  $\sim 20$ –25% of stars form outside clusters.

There is independent evidence, based on simulations of field binary star synthesis rather than on star counts in star forming regions, that the majority of stars formed in clusters (Kroupa 1995). This result applies to stars formed over the lifetime of the Milky Way disk. The similarity between the stellar initial mass function (IMF) inferred from field stars and that measured in young clusters implies that most low mass stars form in clusters, and hence along side massive stars, rather than in an isolated mode, at least in the Milky Way.

Observations of nearby galaxies suggest that a significant fraction of stars form in clusters in these galaxies as well. For example, Meurer et al. (1995) find that 20% of the UV light in seven starburst galaxies they surveyed comes from young star clusters. Similarly, the cluster fraction of the B band light in the galaxy merger NGC 3256 found by Zepf et al. (1999) was 19%, while Fall et al. (2005) found that 20% of the total H $\alpha$  emission in the Antennae galaxies comes from clusters.

In the case of these external galaxies, the estimates of

the cluster fraction ( $\sim 20\%$ ) are likely to be lower limits, a point noted by Fall et al. (2005). For example, Meurer et al. (1995) estimated that the cluster fraction of young stars in NGC 5253 was  $\sim 14\%$  since that fraction of the 2200 Å UV light came from clusters. However, more recent radio and infrared observations of NGC 5253 have revealed the presence of a deeply embedded star cluster, with a luminosity  $\sim 4 \times 10^{42}$  erg s<sup>-1</sup> (Turner et al. 2003), and a correspondingly large ionizing flux  $Q \approx 7 \times 10^{52}$  s<sup>-1</sup> (Turner & Beck 2004) indicating an age of order 1 Myrs or less. This is 43% of the bolometric luminosity of the galaxy, given by Gorjian et al. (2001) as  $9.2 \times 10^{42}$  erg s<sup>-1</sup>, showing that *at least* 43% of the star formation in this galaxy occurs in a single cluster. This extremely luminous cluster was not detected in the UV by Meurer et al. (1995). It seems likely that much of the clustered star formation in starburst galaxies is similarly obscured, so that the clustered star formation estimate of Meurer et al. (1995) is significantly low.

Observations of young star clusters find a power law mass distribution of the form

$$\frac{dN_{cl}(m)}{dm} = N_0 m^{-\alpha} \quad (1)$$

with  $1.5 < \alpha < 2$  in both the Milky Way and in other galaxies (Kennicutt et al. 1989; McKee & Williams 1997). This implies that most massive stars are found in the few most massive clusters. If one believes that massive stars are relevant to galaxy formation, understanding star formation in massive clusters is crucial.

In this paper we show that clusters with initial  $M_{cl} \gtrsim 3 \times 10^6 M_\odot$  were likely supported by radiation pressure just before

<sup>1</sup> Canadian Institute for Theoretical Astrophysics, 60 St. George Street, University of Toronto, Toronto, ON M5S 3H8, Canada; murray@cita.utoronto.ca

<sup>2</sup> Canada Research Chair in Astrophysics

and during the time their stars were forming; it follows that such clusters will exhibit a mass radius relation  $r_{cl} \sim M_{cl}^{3/5}$ , unlike globular clusters, which have radii independent of their masses (by cluster radius we mean the projected radius that encloses half of the cluster light).

In addition, we argue that star formation in massive ( $M_{cl} \gtrsim 10^6 M_\odot$ ) clusters will produce an IMF with a larger characteristic mass than star formation in less massive clusters. The IMF in the Milky Way is described by a broken power law (Kroupa 2001; Muench et al. 2002), or by a log-normal distribution (Miller & Scalo 1979). Similarly, the IMF in young Milky Way clusters such as Orion is described by a broken power, e.g., (Muench et al. 2002), similar to that of the Milky Way as a whole. While the classic Salpeter (1955) IMF has only an upper and lower mass cutoff, these more recent power-law based estimates of the IMF involve at least one additional characteristic mass. In either the log-normal or power-law models, the characteristic mass in the Milky Way is of order  $0.5 M_\odot$ .

The origin of the characteristic mass is disputed in the literature. For example, Adams & Fatuzzo (1996) state that “. . . the Jeans mass has virtually nothing to do with the masses of forming stars”. In contrast, McKee & Ostriker (2007) state “A recurrent theme in star-formation theory is that the characteristic mass—defined by the peak of the IMF—is the Jeans mass at some preferred density.” We argue that the second point of view is correct.

The gas in the interstellar medium is not smoothly distributed; a substantial fraction is found in the form of giant (tens of parsec size and  $10^6 M_\odot$  mass, in the Milky Way) molecular clouds, which contain parsec scale clumps, which in turn contain sub-parsec scale cores; see, e.g., McKee & Ostriker (2007); Bergin & Tafalla (2007). The density increases as one moves down the size and mass scale. The masses typically follow a power law distribution similar in form to that of massive star clusters (eqn. 1 above). This behavior is consistent with the notion that the density and mass distributions are controlled by supersonic turbulence. Both analytic theory and simulations predict log-normal density distributions in the gas density and gas surface density of supersonic turbulent flows; observations find surface densities that are consistent with log-normal distributions.

Measured velocity differences are scale dependent, again consistent with turbulent motions; they are large on large scales, but decrease with decreasing scale. The length scale on which the velocity is equal to the thermal sound speed is called the sonic length. Below this scale turbulent motions cannot compress the gas, so that the density is no longer controlled by turbulence; rather, thermal or magnetic pressure, along with the self-gravity of the gas, will control the density. In the Milky way the sonic length is  $\sim 0.03$  pc. Star forming cores are typically about this size or smaller.

We assume that on scales below the sonic length the fragmentation properties are controlled by the thermal properties of the gas. For an ideal gas equation of state  $P = \rho kT / \mu \sim \rho^\gamma$ , where  $\gamma$  is the effective adiabatic index of the gas. The Jeans mass scales as  $T^{3/2} / \rho^{1/2} \sim \rho^{(3\gamma-4)/2}$ . If  $\gamma < 4/3$  an increase in the gas density (as, for example, when the clump is self-gravitating) leads to a decrease in the Jeans mass and the likelihood of further fragmentation. When  $\gamma > 4/3$  the Jeans mass is an increasing function of density, and so in the ab-

sence of other physics the gas will not fragment. For an isothermal equation of state  $\gamma = 1$ , while for an adiabatic equation of state  $\gamma = 5/3$ .

A hard lower bound to the characteristic mass is given by the opacity limit (Low & Lynden-Bell 1976; Rees 1976), expressed by the condition that the accretion luminosity of a contracting sphere of gas not exceed the black body luminosity of a sphere of the same radius. The critical mass in this case is just the Jeans mass, at the radius and density when the sphere becomes optically thick. This bound applies whether the protostellar core is formed by turbulence and transient, or if it self-gravitates. In either case the luminosity is given roughly by  $L \sim v^5 / G$ ; the velocity is  $v \sim \sqrt{GM/r}$  if the clump is contracting, and larger if it is transient.

Other theories associate the characteristic mass with the Jeans mass at some other density, e.g., with the density at which the gas first becomes thermally coupled to dust grains (Larson 1973, 2005; Jappsen et al. 2005). The argument is that the gas is nearly but not quite isothermal; at low density the temperature decreases with increasing density, but above the critical density temperature begins to increase with increasing density. This is modeled as a change in the effective adiabatic index  $\gamma$  of the gas, from less than unity to slightly more than unity; numerical experiments (Li et al. 2003) indicate that gas fragments readily when  $\gamma < 1$ , but less readily for  $\gamma > 1$ .

Bonnell et al. (2006) perform numerical experiments, using an isothermal equation of state, that show that the mass of the break in the IMF is equal to the initial Jeans mass, and increases with increasing initial Jeans mass. When they employ a Larson style equation of state, they find a fixed characteristic mass in the resulting IMF, corresponding to the density where the adiabatic index suddenly increases from  $\gamma < 1$  to  $\gamma > 1$ .

Competitive accretion (Zinnecker 1982; Bonnell et al. 2001) schemes also predict that the characteristic mass is the mean Jeans mass, i.e., the Jeans mass using the mean density of the star forming region, and  $T \approx 10$  K (Klessen et al. 1998; Bonnell et al. 2006).

Yet other theories for the origin of the IMF start from the notion described above, that the observed fragmentation in giant molecular clouds arises from turbulence, e.g., Padoan & Nordlund (2002). The turbulence establishes a powerlaw in clump mass at the high mass end, with an index similar to the Salpeter values. However, even in this work the *characteristic mass* is related to the Jeans mass (calculated using the mean density) divided by the Alfvén or fast magnetosonic Mach number  $\mathcal{M}_F$  to the  $2/3$  power Padoan & Nordlund (2002), their equation 30.

Elmegreen et al. (2008) note that numerical simulations consistently show a proportionality between the characteristic mass and the thermal Jeans mass, and point out that the observed constancy of the characteristic mass then requires a constant Jeans mass, despite variations in the environments where stars form. We argue below that under conditions found in ultraluminous infrared galaxies (ULIRGs) and other massive galaxies neither the Jeans mass nor the characteristic mass is like that found in the Milky Way.

This paper is organized as follows. In §2 we show how the Jeans mass  $M_J$  varies with cluster mass. When the star forming clumps have  $r_{cl} \sim 1$  pc and  $M_{cl} \gtrsim 10^6 M_\odot$ , the finite optical depth to the far infrared radiation released by the contraction

of the protocluster gas or by the dissipation of turbulent motion leads to an increase in temperature, and, we show, in the Jeans mass. The role of radiation pressure in setting the radius of very massive clusters is described in §3. In §4 we compare our results to observations of massive young clusters, of ultra-compact dwarfs (UCDs) and of central massive objects such as those in Geha et al. (2002) and Walcher et al. (2005). We give a short discussion of our results in the context of previous models for very massive star clusters in §5, and offer our conclusions in §6. In the appendices we discuss the log-normal distribution, the initial mass function (or IMF) that we use and the calculation of the associated light to mass ratio, we outline the calculation of the mass-radius relation for a radiation pressure supported cluster, and finally we discuss the dark matter density on 10 pc scales predicted by recent numerical simulations.

## 2. PROTOCLUSTER FRAGMENTATION AND THE INITIAL MASS FUNCTION

Observations of embedded clusters in the Milky Way show that the star formation efficiency (SFE), the fraction of cluster gas that ends up in stars, is 10–30% (Lada & Lada 2003) for clusters with stellar mass  $\sim 10 - 1000 M_\odot$ . In contrast to this well established result, the time scale over which the gas is converted into stars is nearly as contentious as the the origin of the characteristic mass; it is either the dynamical time, e.g., Elmegreen (2000), or a few to several dynamical times, e.g., Tan, Krumholz & McKee (2006). In appendix A we show that the combination of relatively high SFE and short star formation timescale implies that the initial density of the gas that ends up in stars is no more than a factor  $\rho_m/\bar{\rho} \sim 10$  larger than the mean density  $\bar{\rho}$  of the cluster for rapid star formation; it follows that the Jeans mass of this gas is no less than  $M_J / \langle M_J \rangle \gtrsim 1/3$ , where  $\langle M_J \rangle$  is the Jeans mass calculated using the mean cluster density. For a more extended star-formation time, say 5 dynamical times, and the minimum SFE of 10%, this ratio may be as low as 1/6. Both these estimates are likely to be low compared to reality, since some stars undoubtedly form in less dense but more extended self-gravitating sub-clumps.

The point here is that, while log-normal distributions are broader than gaussians, in the present context they are still rather narrow, so the gas destined for star formation cannot come from too far out on the tail of the density distribution.

Observations of magnetic fields, via Zeeman splitting in OH masers, in both the Milky Way, with  $B \sim 3$  mG (Fish et al. 2003), and in nearby ultraluminous infrared galaxies, also with  $B \sim 3$  mG (Robishaw et al. 2008) indicate that the fast magnetosonic Mach number  $\mathcal{M}_F \lesssim 5$ . Thompson et al. (2006) argue that in ULIRGs the volume average field is also  $\sim 1$  mG, so that the Mach number is globally of the same order.

Simulations suggest that  $\rho_m/\bar{\rho}$  depends only weakly on  $\mathcal{M}_F$  of the turbulence (Ostriker Stone & Gammie 2001). Since the Mach number does not vary over a large range, and assuming that turbulence in the ISM of galaxies is adequately modeled by recent simulations, it follows that the mean Jeans mass of the cluster is a good proxy for the mean Jeans mass of the star forming gas in clusters.

Henceforth we will assume that the characteristic mass is in

fact the Jeans mass of the proto-stellar gas,

$$M_J = \phi_J \left( \frac{\lambda_J}{2} \right)^3 \bar{\rho}, \quad (2)$$

where

$$\lambda_J \equiv \sqrt{\frac{\pi c_s^2}{G \bar{\rho}}} \quad (3)$$

is the Jeans length,  $c_s^2 = kT/\mu m_p$  is the sound speed, and  $\phi_J$  is a dimensionless constant of order unity, accounting for the difference between the mean density of the cluster and the mean density of that fraction of the cluster gas that ends up forming stars.

In a proto-cluster clump of gas, the mean density is given by

$$\bar{\rho} = \frac{3M_{cl}}{4\pi r_{cl}^3}, \quad (4)$$

where  $M_{cl}$  and  $r_{cl}$  are the initial gas mass and radius.

We note that it is likely that both the initial  $M_{cl}$  and  $r_{cl}$  differ from the final cluster mass and radius. For example, we noted that the SFE was of order 10–30%. If the unused gas is expelled on a dynamical time or longer, the cluster will expand by a factor  $\sim 1/SFE$  (Hills 1980) from its original radius. This result is confirmed by numerical simulations (Baumgardt & Kroupa (2007), see their Fig. 4). The simulations show that if the gas is expelled on a shorter time scale, the cluster will expand by a somewhat larger factor, or it may even be destroyed, if the SFE is less than 30%. Baumgardt & Kroupa (2007) show that the final cluster radius will actually be smaller than the initial radius if the cluster is subject to strong tidal forces from its host galaxy.

It is not clear that a cluster with  $M_{cl} = 10^6 M_\odot$  and  $r_{cl} = 3$  pc will have SFE as low as  $\approx 0.3$ . Such a cluster has an escape velocity of order  $50 \text{ km s}^{-1}$ , well above the sound speed of photoionized gas, so any HII region that is formed will be dynamically irrelevant. To see this, note that the dynamical pressure in the cluster is

$$P \approx \pi G \Sigma^2 \approx 8 \times 10^{-6} \text{ g cm}^{-1} \text{ s}^{-2}. \quad (5)$$

Meanwhile, the mean particle number density is  $n \approx 3 \times 10^5 \text{ cm}^{-3}$ , so the pressure of ionized gas is  $P_{HII} = 4 \times 10^{-7} \text{ g cm}^{-1} \text{ s}^{-2}$ , dynamically negligible.

Nor can stellar winds expel the cluster gas; the bolometric luminosity of  $10^6 M_\odot$  of zero age main sequence stars is roughly  $L = 6 \times 10^{42} \text{ erg s}^{-1}$ , while the wind kinetic luminosity is  $L_w \approx 2 \times 10^{40} \text{ erg s}^{-1}$ . The cooling rate of the wind is  $L_{cool} = \Lambda n_h^2 V \approx 10^{42} \text{ erg s}^{-1}$ , where  $V$  is the volume of the cluster and  $n_h \approx 6 \times 10^3 \text{ cm}^{-3}$  is found by assuming the shocked stellar wind has a pressure comparable to the dynamical pressure. In other words, the wind luminosity is not sufficient to produce a pressure high enough to support the weight of the overlying gas. Alternately, the cooling time  $\tau_{cool} = kT/\Lambda n_h \approx 2 \times 10^{10} \text{ s}$  is much shorter than the dynamical time  $\tau_{dyn} = r/v \approx 3 \times 10^{12} \text{ s}$ ; the wind cools before it can push the overlying cold gas out of the cluster.

Supernovae will not remove much gas from the cluster either; the binding energy of the cluster is  $3 \times 10^{52} \text{ erg}$ , about 30 times the kinetic energy supplied by a single supernova.

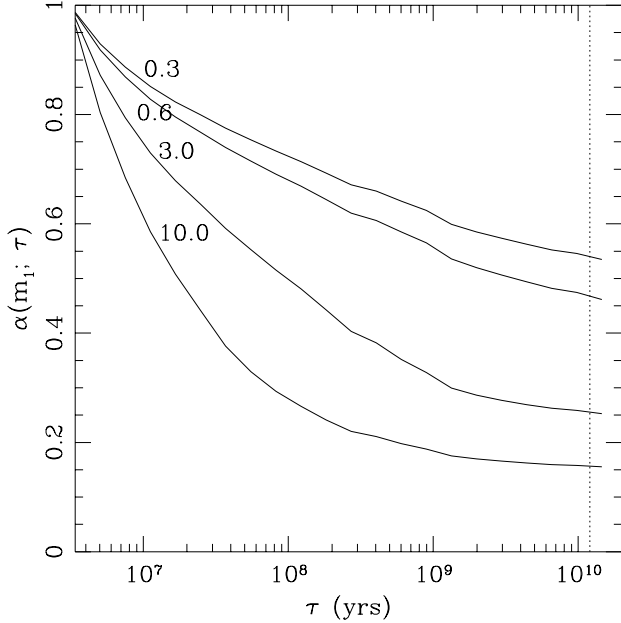


FIG. 1.— The lockup fraction  $\alpha(m_1, z/z_\odot = 0.2; t)$  for the IMF given in equation (B2) and several values of  $m_1$ , as labeled. The vertical dotted line is at 12 Gyrs.

While one expects multiple supernovae to explode, they do not explode all at once. For typical initial mass functions the supernova luminosity is  $L_{SN} \approx 10^{40} \text{ erg s}^{-1}$ , similar to the wind luminosity. Thus supernovae deposit a total energy  $L_{SN} \tau_{dyn} \approx 2 \times 10^{50} \text{ erg}$  in a dynamical time, not sufficient to unbind the cluster (of course the gas cools in less than a dynamical time).

This argument applies to young clusters, with a substantial fraction of their mass in the form of gas. However, for clusters in which the gas fraction is very small, gas removal may be very efficient. For example, in our  $10^6 M_\odot$  cluster, if the gas fraction is reduced to  $1/30$  of the total mass (perhaps because the rest of the mass has been put into stars), the binding energy of the gas is reduced to  $\sim 10^{51} \text{ erg}$ . In that case, a single supernova may be able to eject the gas. Some such mechanism appears to operate in Milky Way globular clusters, as inferred via the following argument: as stars evolve off the main sequence, they lose their envelopes. The mass loss rate from this process would lead to substantial amounts of intercluster gas accumulating, of order  $100 - 1000 M_\odot$  between passages through the plane of the galaxy (Roberts 1988). Observations of the intercluster medium in globular clusters (Freire et al. 2001) show conclusively that this gas does not remain in the cluster, resulting in a net decrease in cluster mass. This reduction in cluster mass is quantified in the so-called lockup fraction  $\alpha(t)$ , the fraction of mass locked up in present day stars and stellar remnants; see, e.g., chapter 7.3 of Pagel (1997). For a Muench et al. IMF with  $m_1 = 0.6 M_\odot$ ,  $\alpha(12 \text{ Gyrs}) \approx 0.45$ , see Figure 1. In our context,  $\alpha(t)$  is a very rough lower limit to  $\epsilon$ .

The Jeans mass associated with a cluster of mass  $M_{cl}$  is set by the temperature  $T$  and the radius  $r_{cl}$ . We examine the Jeans mass in three different cases; 1) when the cluster is either optically thin to far infrared radiation (FIR), or of sufficiently low accretion luminosity that the effective temperature is  $\sim 10 \text{ K}$ ; 2) when the cluster is optically thick and  $T_{eff} \gg 10 \text{ K}$ , but

the cluster is not radiation pressure supported, and 3) when the protocluster gas is radiation pressure supported by the accretion generated luminosity.

To be quantitative, we need to pick a particular IMF. We will use a modified version of the Muench et al. (2002) IMF, described in appendix B and quantified in equation (B2). We consider two modifications to the Muench et al. IMF. The first consists of ignoring the small mass bump (between masses of  $0.025$  and  $0.017 M_\odot$ ), extending the  $0.73$  power law down to the minimum mass we consider, usually  $m_L = 0.1 M_\odot$ . The second modification is that we use a maximum stellar mass of  $M_U = 120 M_\odot$ . Since we ignore the small-mass bump, there are two free parameters (in addition to  $m_L$  and  $m_U$ ) in our IMF, the two break masses  $m_1$  and  $m_2 < m_1$ . Muench et al. find that in the Orion Nebular Cluster,  $m_1 = 0.6 M_\odot$  and  $m_2 = 0.12 M_\odot$ . In this paper we assume that the larger mass is in fact the Jeans mass,  $m_1 = M_J$ .

### 2.1. Optically thin protoclusters

When the protocluster is optically thin to far infrared radiation, as is the case for almost all clusters in the Milky way at the present epoch, the temperature is very nearly independent of cluster radius (or alternately, density); the gas temperature is observed to be around  $10 - 20 \text{ K}$  e.g., Clemens & Barvainis (1988); Rathborne et al. (2006). The Jeans mass is then only dependent on the cluster density. If the mass-radius relation in young Milky Way clusters is taken to be  $r_{cl} \sim M_{cl}^{1/3}$ , which is consistent with the clusters listed in Lada & Lada (2003), the Jeans mass is the same in all current Milky Way protoclusters, and hence (under our assumptions) so is the IMF. This is consistent with observations of the IMF in the Milky Way, except possibly in the galactic center.

For example, consider the best studied young cluster, the Trapezium-ONC cluster in Orion. Hillenbrand (1997) lists 1576 stars, of which 973 are given a probability larger than 0.5 of being members; Hillenbrand gives a lower limit to the stellar mass of  $900 M_\odot$ , which she estimates is about half of the actual mass. Half the stars lie within  $0.72 \text{ pc}$  of the Trapezium, assuming a distance of  $400 \text{ pc}$  to Orion (Kharchenko et al. 2005). The extinction in our direction is small,  $A_v < 2.5$ , while the surface density of stars is currently  $\Sigma = 1800 M_\odot / 1.7 \text{ pc}^2 = 0.2 \text{ g cm}^{-2}$ , corresponding to  $N_H \approx 10^{23} \text{ cm}^{-3}$  and  $A_v \approx 70$ .

As noted above, the star formation efficiency of embedded clusters in this mass range is of order 30% (Lada & Lada 2003). This suggests that the protocluster which formed the ONC had a mass  $\sim 3$  times larger than the current stellar mass. The original dynamical time of the protocluster was  $R/v \sim 10^5 (R/0.7 \text{ pc})(4 \text{ km s}^{-1}/v) \text{ yr}$ , or less, as the original radius was likely smaller than the current radius.

If the gas was removed when it was ionized by the central O stars, its outflow velocity might have been of order  $10 \text{ km s}^{-1}$ , (the sound speed  $c_s \approx 13 \text{ km s}^{-1}$ ) but the pressure of the ionized gas has to overcome the weight of the bulk of the cluster gas. The pressure of the gas was  $\pi G \Sigma^2 \approx 10^{-8} \text{ dynes cm}^{-2}$ , while the pressure of the ionized gas is

$$P_{HII} = \sqrt{\frac{3Q}{4\pi\alpha_{rec}r^3}} kT \approx 10^{-9} \left( \frac{Q}{2 \times 10^{49} \text{ s}^{-1}} \right)^{1/2} \left( \frac{0.72 \text{ pc}}{r} \right)^{3/2} \text{ dynes cm}^{-2}, \quad (6)$$

where  $Q$  is the number of ionizing photons emerging from the O stars per second, and  $\alpha_{rec}$  is the recombination coefficient; we assume photoionization equilibrium. It would appear that initially the ionized gas cannot disrupt the protocluster gas; protostellar jets are a promising candidate for dissipation of cluster gas, but the rate of momentum deposition is such that the removal time is rather long. If so, it is likely that the gas removal was, very roughly speaking, adiabatic.

The original radius of the cluster would then have been  $r \approx 0.24$  pc, while the original mass was  $M \approx 3 \times 2 \times 900 M_\odot = 5400 M_\odot$ . The mean density was  $\rho \approx 6 \times 10^{-18} \text{ g cm}^{-3}$ . The Jeans length  $\lambda_J = 8 \times 10^{16} \text{ cm}$ , and the Jeans mass  $M_J \approx 4 \times 10^{32} \text{ g}$ , or 0.2 solar mass, similar to the value of  $m_1 = 0.6 M_\odot$  found by Muench et al. (2002).

The surface density of the proto-ONC gas was

$$\Sigma \equiv \frac{M}{4\pi r^2} \approx 1.6 \left( \frac{M}{5400 M_\odot} \right) \left( \frac{0.24 \text{ pc}}{r} \right)^2 \text{ g cm}^{-2} \quad (7)$$

as seen from the center of the cluster. This is sufficiently high that we must consider the possibility that the clump was optically thick to far infrared radiation. If we assume  $T = 20 \text{ K}$  is correct, using the Rosseland mean opacity

$$\kappa(T) = 3 \left( \frac{T}{100 \text{ K}} \right)^2 \text{ cm}^2 \text{ g}^{-1} \quad (8)$$

(Semenov et al. 2003) we find  $\tau = 0.2$ . Hence the proto-ONC cloud was optically thin, but only just.

If, on the other hand, we assume the cluster was optically thick, and calculate the accretion luminosity (as is done in the next subsection) we obtain  $T_{eff} = 14 \text{ K}$ , and we still find an optical depth less than unity; we conclude that the ONC was optically thin.

## 2.2. Optically thick protoclusters lacking radiation pressure support

The situation will change if the protocluster is optically thick to far infrared radiation, and if the accretion luminosity is sufficiently high. The temperature of the gas will then be higher than in optically thin clusters, potentially leading to a larger Jeans mass in optically thick clusters. For a metallicity  $Z$  gas the optical depth is

$$\tau = \kappa(T, Z) \Sigma_{cl} \approx 1 \left( \frac{M_{cl}}{2 \times 10^5 M_\odot} \right) \left( \frac{1 \text{ pc}}{r_{cl}} \right)^{-2} \left( \frac{\kappa(100, Z_\odot)}{3 \text{ cm}^2 \text{ g}^{-1}} \right) \left( \frac{T}{100} \right)^2 \left( \frac{Z}{0.1 Z_\odot} \right), \quad (9)$$

where  $\kappa(T, Z)$  is the Rosseland mean opacity, and we have used the fact that  $\kappa(T) \sim (T/100 \text{ K})^2$  for  $T \lesssim 100 \text{ K}$ ; for  $100 \text{ K} < T < 500 \text{ K}$ ,  $\kappa$  is roughly constant.

We have scaled to the properties of a ‘‘metal rich’’ (one tenth solar) Milky Way globular cluster, using a typical present day (stellar) mass but a small half light radius. The reason for the latter choice is that the lockup fraction  $\alpha(t) \approx 0.45$ ; if this mass was lost from the cluster, the radius of the cluster has expanded by a factor of 2.2 since it formed. We noted above that observations of the intercluster medium in globular clusters, e.g., Freire et al. (2001), show that the gas expelled from evolving stars is rapidly removed from the cluster.

If the star formation was less than 100% efficient, the amount of expansion would have been larger.

The heat source that, for massive or compact enough clusters, drives the gas above  $T \approx 10 \text{ K}$  is the contraction of the clump due to its own self-gravity. Consider a clump of mass  $M_{cl}$  and radius  $r_{cl}$ , contracting at roughly its free fall time  $\tau_{ff}$ . The cluster generates a luminosity

$$L_{acc} = \frac{GM_{cl}^2}{r_{cl}\tau_{ff}} = \phi_{ff} \frac{v^5}{G}, \quad (10)$$

where  $\phi_{ff}$  is a dimensionless constant of order unity, and

$$v = \sqrt{\frac{GM_{cl}}{r_{cl}}}. \quad (11)$$

The luminosity of a  $10^6 M_\odot$  cluster with  $r_{cl} = 1 \text{ pc}$  contracting at the free fall rate is

$$L_{acc} \approx 1.9 \times 10^{41} \phi_{ff} \left( \frac{M_{cl}}{10^6 M_\odot} \right)^{5/2} \left( \frac{r_{cl}}{1 \text{ pc}} \right)^{-5/2} \text{ erg s}^{-1}. \quad (12)$$

We stress once again that this luminosity is not related to any star formation.

The effective temperature of the collapsing gas is

$$T_{eff} \approx 17 \phi_{ff}^{1/4} \left( \frac{M_{cl}}{10^5 M_\odot} \right)^{5/8} \left( \frac{r_{cl}}{1 \text{ pc}} \right)^{-9/8} \text{ K}. \quad (13)$$

For  $M_{cl} = 10^5 M_\odot$  this is comparable to the temperature seen in star forming cores in the Milky Way, so we would not expect any change in the IMF.

However, for clusters larger than  $\sim 10^6 M_\odot$ ,  $T \approx 70 \text{ K}$ , and the interior temperature of the protocluster is higher still. To find the run of  $T$  with  $r$ , we solve the radiative transfer equation in the diffusive limit, employing the Rosseland mean opacity as calculated by Semenov et al. (2003). We start at the surface of the clump, with a known luminosity, radius, and effective temperature. Since the clump is nearly in free-fall, we assume the density scales as  $\rho(r) \sim 1/r^2$ . With  $\rho$  and  $T$  known, we can find the opacity. Integrating inwards, we solve for the temperature; then using our prescribed density and the new  $T$ , we find the opacity, and proceed inwards.

Once we know  $T(r)$ ,  $\kappa(r)$ , and (our assumed)  $\rho(r)$ , we calculate a mass weighted temperature. For the parameters used here, we find  $T_{mass} \approx 165 \text{ K}$ , but this varies with the mass and metallicity of the cluster

The corresponding Jeans length is

$$\lambda_{Jeans} \approx 1.4 \times 10^{17} \text{ cm}, \quad (14)$$

while the Jeans mass is

$$M_{Jeans} \approx 2.7 \phi_J M_\odot. \quad (15)$$

Figure 2 plots  $M_J$  as a function of  $M_{cl}$  for three different values of the metallicity. The cluster radius is set to 1.0 pc for  $2000 M_\odot < M_{cl} < M_{cl}^*$ , where  $M_{cl}^* \approx 10^6 M_\odot$  is the mass at which  $r_{cl}$  begins to rise as a result of the increased accretion luminosity, as discussed below in §3. For smaller masses  $r_{cl}$  is chosen to match the present day mean cluster radius in the Milky Way, allowing for cluster expansion as the lockup fraction  $\alpha(t)$  decreases due to stellar evolution.

The Figure shows that  $M_J$  first decreases with increasing  $M_{cl}$ . At small cluster masses, where the cluster is optically thin to FIR radiation, the temperature is independent of  $M_{cl}$ , while the density increases, so  $M_J$  decreases with increasing  $M_{cl}$ . This is a result of our assumption that the initial cluster radius does not vary with cluster mass. This assumption can be checked by measuring the IMF in globular clusters, and seeing if massive clusters show signs of a sharp decrease in the number of stars, binned by mass, as the stellar mass increases. This signature of the IMF may, however, be erased by the combination of mass segregation and preferential evaporation of low mass stars, e.g., (Baumgardt & Makino 2003).

The Jeans mass rather abruptly jumps up (at  $M_{cl} \sim 10^5 - 10^6 M_\odot$ , depending on metallicity); this jump is followed by a rapid but smooth increase. The jump reflects the fact that the cluster has become optically thick; it is artificially abrupt due to our crude treatment of the radiative transfer when the optical depth is near unity. The smooth increase reflects the increase in  $T$  driven by the increase in accretion luminosity with increasing  $M_{cl}$ ,  $T_{eff} \sim M_{cl}^{5/8}$ . Assuming a constant  $r_{cl}$ , we find  $M_J \sim M_{cl}^{7/16}$ .

There is a slight break in the slope at  $M_{cl} \approx 10^6 M_\odot$  (for solar metallicity) related to the increase in  $r_{cl}$  mentioned above and driven by radiation pressure support; at higher  $M_{cl}$  the temperature actually decreases, although very slowly,  $T_{eff} \sim M_{cl}^{-1/20}$ . However,  $M_J$  continues to increase rather rapidly, because the mean density actually decreases,  $\rho \sim M_{cl}^{-4/5}$ . We find  $M_J \sim M_{cl}^{13/20}$ .

We note that the Jeans mass increases rather strongly with increasing cluster mass; this will result in a mass to light ratio  $\Upsilon_V$  that, for old clusters, will also increase with increasing  $M_{cl}$ . We will return to this point below.

### 2.3. Mass to light ratios of clusters with large Jeans masses

The luminosity to mass ratio of the modified IMF will differ significantly from that of the standard Muench et al. IMF; a larger fraction of the resulting young stellar cluster is in massive stars, leading to a higher luminosity to mass ratio. The luminosity to mass ratio as a function of the Jeans mass is shown in Fig. 3 for a cluster with an age of 2.5 Myrs. The horizontal dashed line is the Eddington luminosity to mass ratio,  $4\pi Gc/\kappa_{es}$ , where  $\kappa_{es} \approx 0.38 \text{ cm}^2 \text{ g}^{-1}$  is the electron scattering opacity.

Figure 4 shows the luminosity to mass ratio for the same cluster models shown in Fig. 2. Recall that these models had  $r_{cl} = 1 \text{ pc}$  for  $10^4 M_\odot < M_{cl} < 10^6 M_\odot$ . It is not clear that this is the correct mass-radius relation to use. However, the general trend of a slowly varying  $L/M$  ratio for small mass clusters, with an increase for masses above some value ( $\sim 10^5 M_\odot$  in the Figure) should be correct for the actual mass-radius relation for massive protoclusters.

While these optically thick clusters have high  $L/M$  ratios compared to optically thin clusters when they are young, they have low  $L/M$  ratios, or high  $M/L$  ratios, when they are more than a few Gyrs old, as illustrated by the lines in Figs. 5 and 6. The reason is clear; when young, the cluster luminosity is dominated by massive stars, and optically thick clusters have more massive stars per unit mass (and hence fewer low mass

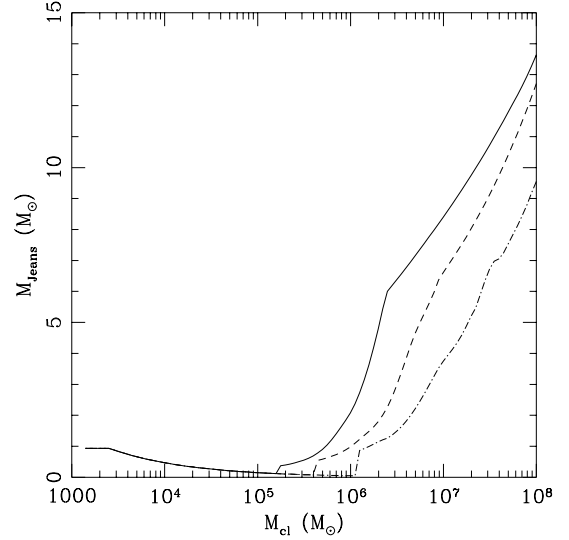


FIG. 2.— The Jeans mass plotted against stellar cluster mass  $M_{cl}$ ;  $M_{cl}$  is the initial gas mass of the proto-cluster, i.e., the plot does not take account of any gas expelled from the cluster as the stars are formed. The metallicities are  $z/z_\odot = 1$  (solid line),  $z/z_\odot = 0.1$  (dashed), and  $z/z_\odot = 0.01$  (dot-dash). The Jeans mass initially decreases with increasing  $M_{cl}$ , since  $T$  is constant while  $\rho$  increases (because we have assumed  $r_{cl}$  is constant for  $2000 < r_{cl} < 10^5 M_\odot$ ); this decrease is halted when the cluster becomes optically thick, leading to an increase in  $T$  and hence in  $M_J$ . The result is a rapid increase in  $M_J$  with increasing  $M_{cl}$ . There is another change in behavior when the protocluster becomes radiatively supported, for  $M_{cl} \gtrsim 10^6 M_\odot$  (depending on metallicity). See text for further details.

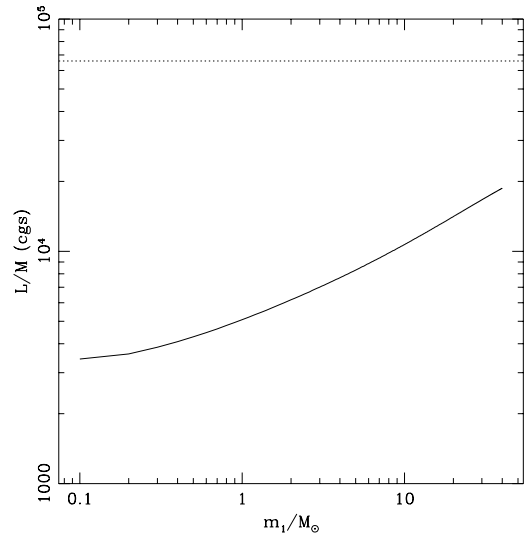


FIG. 3.— The luminosity to mass ratio for a modified Muench et al. IMF, plotted as a function of  $m_1$ , interpreted as a Jeans mass, i.e.  $m_1 = m_J$ . The cluster age is 2.5 Myrs. The horizontal dotted line gives the Eddington ratio  $4\pi Gc/\kappa_{es} = 6.6 \times 10^4 \text{ cm}^2 \text{ s}^{-3}$ .

stars per unit mass) than optically thin clusters. However, after all the massive stars have evolved, the cluster light is supplied by low mass stars, and the optically thin clusters have more  $0.6 - 0.8 M_\odot$  stars per total mass than do the optically thick clusters; the optically thick clusters have more stellar remnants (primarily white dwarfs, with some neutron stars and possibly black holes) than the optically thin clusters.

## 3. RADIATION PRESSURE SUPPORTED PROTOCLUSTERS

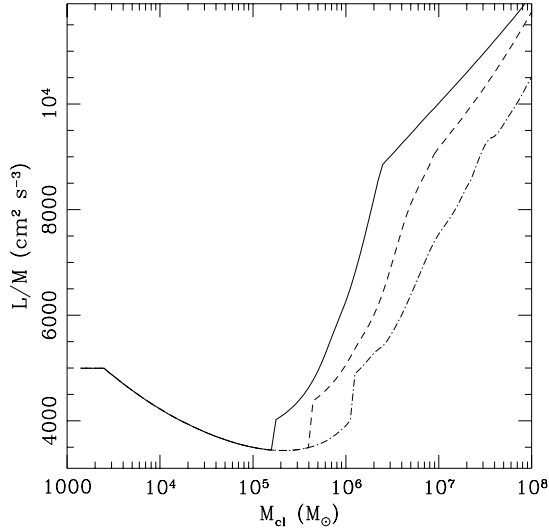


FIG. 4.— The luminosity to mass ratio for the clusters shown in Figure 2, at an age of 2.5 Myr. The jump in  $L/M$  occurs at the mass where the cluster becomes optically thick to the far infrared radiation.

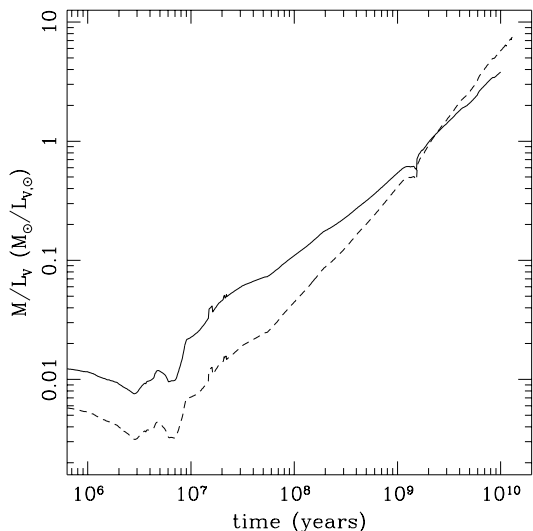


FIG. 5.— The mass to light ratio  $\Upsilon_V \equiv M/L_V$ , in solar units (solar mass over solar v-band luminosity) for an optically thin (solid line,  $m_j = 0.5M_\odot$ ) and an optically thick (dashed line,  $m_j = 10.0M_\odot$ ) cluster as a function of cluster age, as calculated by Starburst99 (Leitherer et al. 1999; Vázquez & Leitherer 2005). The metallicities ( $Z = 0.2Z_\odot$ ) and initial stellar masses of the two clusters are the same. When the clusters are young, the optically thick cluster is more luminous than the optically thin cluster, but after a few gigayears the optically thin cluster is more luminous than the optically thick cluster.

Another dramatic change occurs when the protocluster is massive enough that the accretion luminosity is dynamically important. The protocluster has an FIR optical depth larger than one, so the outward force exerted by the radiation is

$$F = \frac{\tau L_{\text{acc}}}{c}. \quad (16)$$

If this force is less than that of gravity, the protocluster will continue to shrink, but as  $r$  decreases the radiation force increases as  $r^{-9/2}$ , while the force of gravity increases as  $r^{-2}$ . For small enough  $r$  the radiation pressure overcomes the force of gravity and the collapse is slowed.

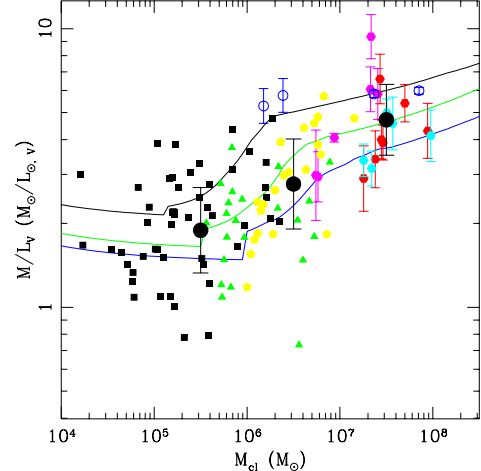


FIG. 6.— The mass to light ratio  $\Upsilon_V = M/L_V$  as a function of dynamical mass  $M_{cl}$ . The squares are Milky Way globular clusters (Harris (1996); velocities from Pryor & Meylan (1993)). Triangles are M31 globular clusters (for which velocity dispersions are available) from Barmby et al. (2007). The filled pentagons are globular clusters near NGC 5182 (Cen A) from Rejkuba et al. (2007). The filled hexagons are UCDs from Hasegan et al. (2005) (magenta), Virgo UCDs from Evstigneeva et al. (2007) (red), and Fornax UCDs (Hilker et al. 2007) (cyan). The open blue circles are the nuclei of Virgo dwarf elliptical galaxies from Geha et al. (2002). The large filled circles are the mean  $\Upsilon_V$  in three mass bins  $M_{cl} < 10^6 M_\odot$ ,  $10^6 M_\odot < M_{cl} < 10^7 M_\odot$ , and  $10^7 M_\odot < M_{cl}$ . The mass to light ratios of all clusters have been adjusted for the effects of two body relaxation and tides, as described in the text. The solid lines give the predictions of equations (2), (13), and (17) for a solar metallicity cluster (top curve), for a metallicity of 0.2 solar (middle curve), and a metallicity of 0.02 solar, all at an age of 10 Gyrs.

The optical depth  $\tau$  is measured from the center of the protocluster outward. Equation (16) assumes that the optical depth is independent of direction, which is not strictly speaking true given the turbulent nature of the cluster gas. The optical depth is proportional to the column density of gas. The column density distribution has been measured in the Milky Way by a number of authors, e.g., Goodman, Pineda, & Schnee (2008) or Wong et al. (2008), and has been found to be consistent with a log-normal distribution. Numerical simulations also find log-normal surface density distributions (Ostriker Stone & Gammie 2001). The observations measure  $\tau$  along the line of sight from the Earth through the cloud rather than from the center of the cloud outward, but the two surface density distributions should not differ dramatically. In the notation of appendix A, Goodman, Pineda, & Schnee (2008) find  $0.11 < \sigma < 0.22$ , corresponding to  $0.01 < \mu < 0.05$ . This agrees well with the results of Ostriker Stone & Gammie (2001).

For  $\mu = 0.05$ , 99% of sight lines have  $\tau/\bar{\tau} > 0.2$ , where  $\bar{\tau}$  is the (angular) mean of the optical depth. Since  $\bar{\tau} \approx 50$  for  $M_{cl} = 10^6 M_\odot$  and  $r_{cl} = 1$  pc, there are essentially no optically thin sight lines for such massive clusters. In fact, the radiation pressure does not become dynamically important until the cluster is smaller than 1 pc and  $\bar{\tau}$  is larger, but this only decreases the chance that photons leak out in directions with small optical depth.

When the radiation force approaches that of gravity, the collapse will slow from the free fall rate to the Kelvin rate. In

appendix C we show that this occurs at a radius

$$r_{\text{rad}} = \phi_{\text{rad}} G^{1/5} \left( \frac{\kappa}{4\pi c} \right)^{2/5} M_{\text{cl}}^{3/5} \approx 1.5 \times 10^{18} \left( \frac{M_{\text{cl}}}{10^6 M_{\odot}} \right)^{3/5} \left( \frac{\kappa}{3 \text{ cm}^2 \text{ g}^{-1}} \right)^{2/5} \left( \frac{\phi_{\text{rad}}}{3} \right) \text{ cm}. \quad (17)$$

It can be shown that this is also the radius at which the photon diffusion time out of the clump is equal to the clump dynamical time.

These radiation supported clusters have a monotonically increasing  $r_{\text{cl}}(M_{\text{cl}})$  relation, unlike the less massive globular clusters found in the Milky Way and other nearby galaxies. This will change a number of their properties. For example, their surface densities will *decrease* with increasing mass,

$$\Sigma(M_{\text{cl}}) = 70 \left( \frac{M_{\text{cl}}}{10^6 M_{\odot}} \right)^{-1/5} \left( \frac{\kappa}{3 \text{ cm}^2 \text{ g}^{-1}} \right)^{-4/5} \left( \frac{\phi_{\text{rad}}}{3} \right)^{-2} \text{ g cm}^{-2}, \quad (18)$$

where we use  $\Sigma \equiv M/(4\pi r^2)$ . This scaling with cluster mass is in contrast to globular clusters, which have surface densities that increase with  $M_{\text{cl}}$ ,  $\Sigma(M_{\text{cl}}) \sim M_{\text{cl}}$ . The volume density will decrease even more rapidly

$$\rho(M_{\text{cl}}) \sim M_{\text{cl}}^{-4/5}. \quad (19)$$

This will have consequences for the evolution of binary systems, in particular the precursors to LMXBs and millisecond pulsars. Since the formation of such binaries depends strongly on the stellar number density, the number of LMXBs and millisecond pulsars per stellar mass will peak at a cluster mass  $\sim 3 \times 10^6 M_{\odot}$ .

The escape velocity will also behave differently for the more massive clusters,

$$v(M_{\text{cl}}) \approx 93 \left( \frac{M_{\text{cl}}}{10^6 M_{\odot}} \right)^{1/5} \left( \frac{\kappa}{3 \text{ cm}^2 \text{ g}^{-1}} \right)^{-1/5} \left( \frac{\phi_{\text{rad}}}{3} \right)^{-1/2} \text{ km s}^{-1} \quad (20)$$

compared to the much more rapid  $v(M_{\text{cl}}) \sim M_{\text{cl}}^{1/2}$  for globular clusters.

It follows that the accretion luminosity  $L \sim M_{\text{cl}}$  as expected (assuming  $\kappa$  is constant) since the cluster is limited by the Eddington luminosity. Furthermore, the effective temperature will actually decrease with increasing cluster mass, although very slowly,  $T_{\text{eff}} \sim M_{\text{cl}}^{-1/20}$ .

The stellar luminosity is another question. When the stars ignite, they will increase the luminosity of the cluster. This will tend to increase the radiation pressure, and in turn the radius of the cluster. However, as soon as  $r$  begins to increase, the accretion luminosity will drop so as to maintain the total luminosity near the Eddington value. If the stellar luminosity exceeds the cluster Eddington value, the stars may expel any remnant gas on a dynamical time.

However, the maximum stellar luminosity depends on the IMF, and is generally well below the accretion luminosity, as we now show. The accretion luminosity to mass ratio is

$$\frac{L_{\text{acc}}}{M_{\text{cl}}} = \frac{4\pi G c \kappa_{\text{es}}}{\kappa_{\text{es}} \kappa_{\text{d}}}. \quad (21)$$

The first factor on the right hand side of this equation is the Eddington light to mass ratio,  $(L/M)_{\text{Edd}} = 6.6 \times 10^4 \text{ cm}^2 \text{ s}^{-3}$ ,

while the opacity ratio ranges from 0.1 for solar metallicity dust (and  $T \approx 100\text{K}$ ) to 10 for a low metallicity cluster. From Figure 3 or 4 the maximum stellar  $L_*/M_* \approx 2 \times 10^4 \text{ cm}^2 \text{ s}^{-3}$ , i.e., about 1/3 of the Eddington  $L/M$  ratio. Only for the most massive and metal rich clusters will the stellar luminosity approach (or slightly exceed) the accretion luminosity. However, the largest clusters actually have lower temperatures, as we have just seen, so  $\kappa_{\text{d}}$  is likely to be a bit lower than the rough estimate  $\kappa = 3$  we used here. We conclude that the stellar luminosity is lower than the accretion luminosity, at least until most of the gas has turned into stars.

This assumes that no other mechanism can eject gas from the cluster. One mechanism that might do so is a combination of protostellar jets and stellar winds. Recall that the Jeans mass is of order  $5 - 10 M_{\odot}$  in these clusters, so a substantial fraction of stars will have massive winds. Both the protostellar winds and jets will have mechanical luminosities less than a tenth of the stellar Eddington luminosity. These winds and jets will shock, producing gas at  $T = 10^9 \text{ K}$ , but this gas will rapidly cool by conduction to  $T \approx 10^7 \text{ K}$ . From that temperature it will cool radiatively in a time of order  $10^4$  years, less than a dynamical time, as we showed above in §2. We tentatively conclude that jets and winds will not expel the bulk of the cluster gas.

Given that observed clusters are only a factor of a few times larger than the minimum radius allowed by radiation pressure, it would appear that the fraction of gas ejected may be of order 1/2, but not substantially larger. We leave this question for later work.

As with the optically thick accretion heated clusters discussed in §2.2, the IMF of these clusters will be top heavy, with Jeans masses ranging up to  $10 M_{\odot}$ , as shown in Fig. 2. When they are young, they will have elevated light to mass ratios; when older, their mass to light ratios will be higher than ordinary optically thin globular clusters of the same age and metallicity; see Figure 6 and the next subsection.

The very high  $m_{\text{J}}$  predicted by these models suggests that the lockup fraction  $\alpha(t)$  will be particularly small for these very massive clusters, perhaps as small as 0.3 or less (Fig. 1). We have noted above that the gas expelled from evolving stars is rapidly removed from present day globular clusters (Freire et al. 2001). The escape velocity from the more massive clusters considered here is only slightly higher than in globulars, so the same gas removal mechanism, whatever it is, should be effective. The radius of a cluster of age  $\tau$  will then depend on the *present day* stellar mass as

$$r_{\text{cl}}(\tau, M_{\text{cl}}) = \alpha(\tau)^{-8/5} \phi_{\text{rad}} G^{1/5} \left( \frac{\kappa}{4\pi c} \right)^{2/5} M_{\text{cl}}^{3/5}. \quad (22)$$

This relation is shown as the dashed line in Figure 8 for  $\alpha(t) \approx 0.38$ , appropriate for a 10 Gyr old cluster with a Jeans mass of  $2 M_{\odot}$ .

If these massive clusters have larger Jeans masses than optically thin globular clusters, they will experience a larger relative expansion in  $r_{\text{cl}}$  than the globular clusters. Evidence for this expansion may be detectable in old massive clusters as a surrounding halo of stars extending out to the tidal radius; both the larger relative expansion and the larger number of stars in the massive clusters will render this halo more visible than similar halos around globulars.

The small lockup fraction will also alter the present day

values of derived quantities such as surface density, relative to the initial values give above. For example, the surface densities will be smaller by  $\alpha^3$ , as illustrated by the dashed line in Figure 9.

### 3.1. The relation between luminosity and velocity dispersion in massive old clusters

We noted above that the mass to light ratio  $\Upsilon_V$  will be an increasing function of cluster mass, even at fixed metallicity. This will lead to a relation between luminosity and velocity dispersion that differs from that expected from a simple application of the virial theorem,  $L \sim \sigma^5$ .

We start with the observation that the luminosity of a cluster depends on the IMF, or, in our case on the Jeans mass. Consider an old cluster, in which the turnoff mass (the main sequence lifetime of a star at the turnoff mass is equal to the age of the cluster) is smaller than the Jeans mass. The mass to light ratio of such a cluster is an increasing function of the Jeans mass; the cluster light is coming from stars on the flat part of our adopted IMF, and the number of such stars (at a fixed initial cluster mass) decreases with increasing  $M_J$ . Another way to say this is that a larger  $M_J$  leads to more mass in massive stars, which contribute no light at late times, leaving less mass in (and fewer numbers of) low mass stars to illuminate the cluster's declining years. Hence  $\Upsilon_V = M_{cl,i}/L_V$ , where the subscript  $i$  denotes the initial cluster mass, increases with increasing  $M_J$ . The mass to light ratio for our IMF scales as  $\Upsilon_V(M_J) \sim M_J^{0.73}$ , as long as the turnoff mass is below  $M_J$ .

The observationally accessible quantity is  $\Upsilon_V(M_{cl})$ ; we measure the present day cluster mass, not the initial cluster mass. For clusters with  $T_{eff} > 10K$  (optically thick clusters with sufficiently high accretion rates to heat the gas, but not to provide radiation support) we can estimate the scaling  $\Upsilon_V(M_{cl,i}) \sim M_{cl,i}^{0.32}$ . The exponent is 0.73 times 7/16, the latter arising from the scaling relation between  $M_J$  and the initial  $M_{cl}$ ,  $M_J(M_{cl,i}) \sim M_{cl,i}^{7/16}$ , found in §2.2. The present day  $M_{cl}$  is smaller than  $M_{cl,i}$  by (at least) a factor  $\alpha$ . Given  $M_{cl,i}$ , we can calculate  $M_J$  and hence  $\alpha$ , whence we can find the present day  $M_{cl}$ . Doing so, we find

$$\Upsilon_V(M_{cl}) \sim M_{cl}^{0.28}, \quad (23)$$

The situation for radiation supported clusters is similar, but the Jeans mass varies more rapidly with the initial cluster mass,  $M_J \sim M_{cl,i}^{13/20}$ . This occurs despite that fact that the effective temperature of the cluster actually decreases with increasing  $M_{cl}$ ; the decreasing temperature is more than offset by the rapidly increasing cluster radius (or decreasing density). The result is  $\Upsilon_V(M_{cl}) \sim M_{cl,i}^{0.47}$ , and

$$\Upsilon_V(M_{cl}) \sim M_{cl}^{0.11}. \quad (24)$$

Using the scaling of mass to light ratio  $\Upsilon_V$  with cluster mass  $M_{cl}$ , we can find the relation between the stellar luminosity and the cluster velocity dispersion  $\sigma \equiv v/\sqrt{\Gamma_{vir}}$ , where the constant  $\Gamma_{vir}$  is defined by  $M_{vir} = \Gamma_{vir}\sigma^2 r_{cl}/G$ . We start with

$$L_V = 5 \times 10^5 L_{V,\odot} \left( \frac{2}{\Upsilon_{V,6}} \right) \left( \frac{M_{cl}}{10^6 M_\odot} \right)^{0.89}, \quad (25)$$

where  $\Upsilon_{V,6}$  is the mass to light ratio for a cluster of  $10^6 M_\odot$ .

Combining this with equation (20) we find

$$L_V = 1.6 \times 10^6 L_{V,\odot} \left( \frac{\sigma}{20 \text{ km s}^{-1}} \right)^{4.45} \left( \frac{\alpha(10 \text{ Gyrs})}{0.38} \right)^{4.45} \left( \frac{2}{\Upsilon_{V,6}} \right) \quad (26)$$

for the present day luminosity of a radiation pressure supported cluster formed 10 Gyrs ago. For optically thick clusters that were not radiation pressure supported,  $L_V \sim \sigma^{3.6}$ .

## 4. COMPARISON WITH OBSERVED CLUSTER PROPERTIES

We start by considering the light to mass ratio  $L/M$  for young clusters, then the mass to light ratio  $M/L$  for old clusters<sup>3</sup>. Either ratio is affected by a number of parameters, including age, IMF, and metallicity. A cluster's  $L/M$  depends most strongly on age, moderately weakly on the IMF (for the type of model considered in this paper), and very weakly on metallicity.

Figure 5 shows that  $M/L$  varies by a factor of several hundred over 10 Gyrs for a given  $M_{cl}$  and metallicity. Figure 6 shows that over the observed range of cluster masses, variations in the Jeans mass should produce a variation in the mass to light ratio (at 10 Gyrs) from  $\sim 2M_\odot/L_{V,\odot}$  at  $M_{cl} = 10^5 M_\odot$  to  $\sim 6$  at  $M_{cl} = 10^8 M_\odot$ , in increase of more than a factor of 3.

The metallicity of a cluster affects the  $\Upsilon_V$  of a cluster with a fixed IMF, since main sequence metal poor stars of a given mass tend to be more luminous than metal rich stars of the same mass and age. However, the effect is not strong: Figure 6 shows that a factor of five change in metallicity changes  $M/L_V$  (at an age of 10 Gyrs) by about 42% around  $M_{cl} = 10^6 M_\odot$ , but by only 20% near  $M_{cl} = 10^8 M_\odot$ . Since the metallicity can be obtained with moderate precision from spectroscopic studies of a cluster, this direct source of variation in  $M/L$  is reasonably easy to account for.

The metallicity can also indirectly affect our estimate of  $M/L$ . For example, Jordan (2004) has pointed out that high metallicity clusters can appear to have smaller half light radii than low metallicity clusters of the same age, mass, and IMF; the mass of turnoff stars (which dominate the light of the cluster) is smaller in the metal poor cluster than that in the metal rich cluster. The variation in radius is  $\sim 20\%$  for a factor of ten variation in metallicity, and the change in the apparent mass is of the same order.

We conclude that clusters with  $M_{cl} \approx 10^8 M_\odot$  should have  $M/L_V \approx 6$  or higher, more than a factor of two higher than globular clusters, and that metallicity variations cannot produce such a large change in  $M/L_V$ . Armed with these results, we proceed to examine various clusters for evidence of a top-heavy IMF.

### 4.1. The light to mass ratio of young clusters

In M82 the luminosities, ages, and projected half light radii of a number of star clusters have been measured (Smith & Gallagher 2001; McCrady et al. 2003; Smith et al. 2006); the first two papers also measured line of sight velocity dispersions for a total of three clusters. The line of sight velocity dispersions for 19 clusters have been measured by McCrady & Graham (2007).

<sup>3</sup> We reverse the ratio with advancing age since this is the practice in the literature

Both Smith & Gallagher (2001) and McCrady et al. (2003) present evidence that cluster M82-F has a luminosity (in the F160W filter) to mass ratio about a factor of  $\sim 2.5$  higher than expected for a cluster of its estimated age ( $\sim 50$  Myrs). They suggest a lower mass cutoff to the IMF of  $2.5M_{\odot}$  and  $\sim 1M_{\odot}$ , respectively. The projected half light radius and mass of M82-F are  $r_{cl} = 89$  mas, about 1.5 pc at 3.6 Mpc, the distance to M82, and  $M_* = 5.5 \times 10^5 M_{\odot}$ . Using these values, and a metallicity 1.7 times solar, we find that the Jeans mass in M82-F is  $\sim 2.5M_{\odot}$ .

The status of M82-F is the subject of some debate in the literature; see Bastian et al. (2007) for an extended discussion of this object. These authors find a high  $\Upsilon$ , as have previous authors. They offer several possible explanations, including a top-heavy IMF, but also mass segregation (not seen with their data) and inaccurate estimates of the velocity dispersion resulting from spatially variable extinction. They rule out the suggestion of Bastian & Goodwin (2006) that M82-F is younger than 20 Myrs.

Similarly, McCrady et al. (2003) find that their cluster 11, with  $r_{hp} = 1.2$  pc and  $M_* = 3.5 \times 10^5 M_{\odot}$ , has  $L/M$  about 2.5 times larger than expected, again suggesting a top heavy IMF. Any mass segregation in this cluster would have to be primordial, since the cluster is so young, around 10 Myrs. For this cluster, our models predict a Jeans mass of  $2.3M_{\odot}$ .

In contrast to these results for clusters M82-F and M82-11, McCrady et al. (2003) and McCrady & Graham (2007) find that their cluster 9 has  $r_{hp} = 2.6$  pc and  $M_* = 2.3 \times 10^6 M_{\odot}$ . This cluster has  $L/M$  consistent with a normal IMF, while our models predict a large Jeans mass and a high  $L/M$  ratio.

The other clusters in M82 are optically thin, so we do not expect them to have elevated  $L/M$  ratios.

Both Smith & Gallagher (2001) and McCrady et al. (2003) consider the effects of mass segregation (heavier stars either forming preferentially or settling into the cluster center). Smith & Gallagher (2001) argue that this is unlikely to explain the higher  $L/M$ , while McCrady et al. (2003) are more circumspect.

Boily et al. (2005) find that the dynamically evolving mass segregation will cause the half light radius to decrease, weakening the argument for an enhanced light to mass ratio in M82-F, but not in cluster 11 (due to its youth, dynamical mass segregation is not important in this cluster).

Moving to young superstar clusters in galaxies other than M82, Bastian et al. (2006) list eleven clusters less than 300 Myrs old; of these only NGC 4038:W99-15 is optically thick. Like M82:9, this cluster has a light to mass ratio consistent with a normal IMF. Other massive clusters listed in Bastian et al. (2006), such as NGC7252:W3, NGC7252:W30 and NGC 1316:G114, which are optically thick, are between 500Myr and 3Gyrs old (Bastian et al. 2006), so they are also not expected to have elevated  $L/M$  ratios (see Fig. 5).

To summarize, we are aware of only four young (less than 300Myr old) clusters in the literature that were probably born optically thick to far-infrared radiation, M82-F, M82-11, M82-9, and NGC 4038:W99-15. The first two show signs of having elevated light to mass ratios, while the latter two do not.

#### 4.2. The mass to light ratio of massive star clusters

Figure 6 shows observed mass to light ratios for several classes of star clusters, including globular clusters from the Milky Way, M31, and Cen A, more massive UCDs from the Virgo and Fornax clusters, and four nuclei of Virgo dwarf ellipticals. Where available we have used masses from the literature obtained by fitting models to individual clusters. Where such detailed fits are not available, we have calculated the masses from the observed velocity dispersions  $\sigma$  and half light (or effective) radii  $r_{cl}$  using the expression

$$M = \Gamma_{vir} \frac{\sigma^2 r_{cl}}{G}. \quad (27)$$

We use  $\Gamma_{vir} = 10$ . We use only objects for which the quoted error for  $\sigma$  is less than half the value of  $\sigma$ .

Binning the clusters by mass ( $M_{cl} < 10^6 M_{\odot}$ ,  $10^6 < M_{cl} < 10^7 M_{\odot}$ , and  $10^7 M_{\odot} < M_{cl}$ ), we find  $\Upsilon_V = 1.9 \pm 0.8$ ,  $2.8 \pm 1.2$ , and  $4.7 \pm 1.6$  respectively, all in solar units, consistent with the impression given by the points representing individual objects. This rapid increase in  $\Upsilon$  with increasing cluster mass (or luminosity) has been noted previously, e.g., by Hasegan et al. (2005).

The mass to light ratio  $\Upsilon$  of a cluster changes with age due to both stellar evolution and to differential loss of low mass compared to high mass stars. The latter is a result of two body relaxation combined with tidal stripping, e.g., Baumgardt & Makino (2003). As Fig. 5 shows, the effect of stellar evolution is to increase  $\Upsilon$  with increasing cluster age. The solid curves in Fig. 6 assume that the clusters are 10 Gyrs old. Some of the UCDs may well be this young or younger; if they are younger, their  $\Upsilon$  values should be increased slightly to compare to the globular clusters, since the latter almost certainly are 11–12 Gyrs old.

Metallicity also affects  $\Upsilon$ , but the majority of the objects plotted in the figure, including the UCDs, have  $[\text{Fe}/\text{H}] < -1$ . It is worth stressing that for such low metallicities both the Kroupa and Muench et al. IMFs predict  $\Upsilon_V < 3$  for these low metallicities.

##### 4.2.1. Dynamical effects

Variations in  $\Upsilon$  due to relaxation and tides are most relevant for low mass objects. Relaxation initially reduces  $\Upsilon$  as low mass stars are tidally stripped from the outskirts of the cluster, then increases  $\Upsilon$  just before the cluster is disrupted at time  $T_{dis}$ . The disruption time found by the numerical simulations is well approximated by (Baumgardt & Makino 2003)

$$T_{dis} = \beta \left[ \frac{N_*}{\ln(\gamma N_*)} \right]^x \frac{R_G}{\text{kpc}} \frac{220 \text{ km s}^{-1}}{v_c} (1 - \varepsilon), \quad (28)$$

where the values of the constants are  $\beta \approx 1.9$ ,  $\gamma \approx 0.02$ , and  $x \approx 0.75$ . The cluster is assumed to orbit at a mean radius  $R_G$  from the center of the galaxy on an orbit with eccentricity  $\varepsilon$ . The galaxy has a circular velocity  $v_c$  (or a velocity dispersion which can be converted to an equivalent circular velocity in the case of elliptical hosts). The initial number of stars  $N_* = M_{cl}/\langle m \rangle$ , where  $\langle m \rangle$  is the mean stellar mass for the chosen IMF.

The cluster mass at time  $T$  is related to the initial cluster mass  $M_{cl,i}$  by

$$M_{cl}(T) = 0.70 M_{cl,i} (1 - T/T_{dis}). \quad (29)$$

From Baumgardt & Makino (2003) (their Figure 14) we approximate

$$\Delta\Upsilon \approx \Gamma \left( \frac{T}{T_{dis}} \right), \quad (30)$$

where  $0.3 \lesssim \Gamma \lesssim 0.7$ . From the observed cluster mass (i.e.,  $M_{cl}(T)$ ) we solve equations (28) and (29), then use equation (30) to find  $\Delta\Upsilon$ . Where the eccentricity of the globular cluster orbit is unknown (the majority of the cases) we assume  $\varepsilon = 0.5$ .

In producing Fig. 6 we have increased the mass to light ratio of all the clusters by the appropriate amounts, using  $\Gamma = 0.7$ ; the only noticeable change (typically of order 10–30%) is that suffered by the Milky Way globulars, since they are the least massive and hence have the shortest  $T_{dis}$ . However, even for Milky Way clusters the effect is not large, and neglecting this correction does not alter the qualitative appearance of the figure.

There are recent high precision measurements of the present day mass function (MF) in two globular clusters, M4=NGC 6121 (Richer et al. 2004) and NGC 6397 (Richer et al. 2008). These were chosen for very long HST observations partly based on the fact that they are the two nearest globular clusters.

The metallicity of NGC 6397 is  $[\text{Fe}/\text{H}] = -2.03$  (Gratton et al. 2003), while the age of the cluster is 11.4 Gyrs (Richer et al. 2008). Using  $m_V = 5.73$  and  $r_h = 2.33'$  (Harris 1996), the error-weighted mean velocity dispersion  $\sigma = 3.5 \pm 0.2 \text{ km s}^{-1}$  (Pryor & Meylan 1993), and distance modulus  $m-M = 12.1 \pm 0.1$  or  $D = 2.6 \pm 0.1 \text{ kpc}$  (Richer et al. 2008), the dynamical mass to light ratio of NGC 6397 is  $\Upsilon_V = 1.6 \pm 0.2$  in solar units. This is marginally consistent with a Muench et al. stellar model with that age and metallicity, ( $\Upsilon_V = 1.96$ ) or for a Kroupa IMF ( $\Upsilon_V = 2.1$ ).

Using data from Richer et al. (2004) we find  $\Upsilon_V = 1.2 \pm 0.1$  for M4, too low to be consistent with either type of IMF, but consistent with a maximal amount of dynamical evolution, i.e.,  $\Gamma = 0.7$  and an age approaching the cluster disruption age.

Applying the correction for preferential loss of low mass stars to NGC 6397 we find  $\Upsilon_V = 2.1$ , while for M4 we find  $\Upsilon_V = 1.5$ , the latter now being marginally consistent with the Muench et al. IMF. This suggests that M4 is more dynamically evolved than our application of the (Baumgardt & Makino 2003) would indicate.

The present day mass functions of both these clusters can be fitted by a single power law  $dN/dm \sim m^{-\alpha}$  with  $\alpha = 0.1$ , compared to the Salpeter value 2.35 or the Muench et al. value 1.15 (for masses below the break mass). This is reminiscent of the findings of Baumgardt & Makino (2003), who predict that the MF of evolved clusters will be very flat. However, the simulations predict  $\alpha \approx 0$  only when 90% of the cluster lifetime has passed. It seems somewhat unlikely that the first two clusters examined (chosen for their proximity to us) should both be so near their demise. The rather modest dynamical evolution needed to explain the slightly low  $\Upsilon_V$  for NGC 6397, coupled with the very low  $\alpha$ , suggests some primordial mass segregation in that object.

#### 4.2.2. Non-baryonic dark matter?

The high  $\Upsilon_V \sim 6$  seen in some UCDs studied by Hasegan et al. (2005) led them to suggest that their objects might contain a mass in non-baryonic dark matter comparable to their stellar mass. This suggestion is motivated by the following argument. The mean  $\Upsilon_V \approx 2.0 \pm 0.9$  for Milky Way globulars, using dynamical masses corrected for the preferential loss of low mass stars using eqns. (28), (29), and (30) (as noted above, uncorrected values of  $\Upsilon_V$  are about 20% lower on average). In contrast,  $\Upsilon_V \approx 4.7 \pm 1.5$  for  $M_{cl} > 10^7 M_\odot$ . As mentioned above, most of the more massive objects have  $[\text{Fe}/\text{H}] < -1$ , so neither Kroupa nor Muench et al. IMFs can match the observations. Many of the UCDs appear to have somewhat younger stellar populations than do the globulars, adding to the difficulty.

Possible explanations for different values of  $\Upsilon_V$  include problems with the estimate of the mass to light ratios (e.g., poorly measured velocity dispersions), dynamical effects such as the preferential loss of low mass stars, changes in the IMF associated with increasing cluster mass, or the presence of dynamically significant amounts of non-baryonic dark matter in the more massive clusters. In the latter case, the dark matter would have to have a mass 1.3 times larger than the baryonic matter inside  $r_{cl}$  in cluster with  $M_{cl} > 10^7 M_\odot$ , assuming an IMF that is the same as that in Milky Way globular clusters. In other words, the massive clusters and UCDs would have to be dark matter dominated inside  $\sim 10 \text{ pc}$ .

Given what little we know regarding dark matter, this is unlikely, as we now show.

Figure 7 shows the density of the same objects shown in Fig. 6.

If non-baryonic dark matter is responsible for the elevated mass to light ratios of clusters with  $M_{cl} \sim 10^7 M_\odot$ , it must have a density  $\gtrsim 10^{-19} \text{ g cm}^{-3}$ , or  $1000 M_\odot \text{ pc}^{-3}$  on scales of order 10 pc.

We have examples of dark matter dominated objects for which the density is well measured, namely Milky Way dwarf spheroidal galaxies. These objects have stellar velocity dispersions ranging from  $\sigma = 4 \text{ km s}^{-1}$  to  $27.5 \text{ km s}^{-1}$ , the latter corresponding to the LMC. The crosses in Fig. 7 show the central densities

$$\rho_c = \frac{166\sigma^2}{r_c^2} M_\odot \text{ pc}^{-3} \quad (31)$$

of Milky Way dwarf spheroidal galaxies as tabulated by Madau et al. (2008). In this expression  $r_c = 0.64 r_{cl}$  is the core radius of the stellar light (recall that  $r_{cl}$  is the projected half light radius).

The highest density Milky Way satellite galaxies currently known, Willman 1 and Coma Berenices, have  $\rho = 10^{-21} \text{ g cm}^{-3}$  and  $10^{-22}$  respectively, a factor of one hundred to one thousand below the mean density of the compact  $M_{cl} = 10^7 M_\odot$  clusters. More massive dwarf galaxies have much lower mean (core) densities, typically  $\rho \sim 10^{-23} \text{ g cm}^{-3}$ ; all these dark matter densities are far too small to explain the high densities seen in compact clusters.

The two highest density satellite galaxies (Willman 1 and Coma Berenices) are also the most compact Milky Way galaxies, with  $r_c = 13 \text{ pc}$  and  $41 \text{ pc}$ , respectively. This raises the possibility that the larger satellites have higher densities at radii smaller than  $r_c$ , as expected on theoretical grounds. In

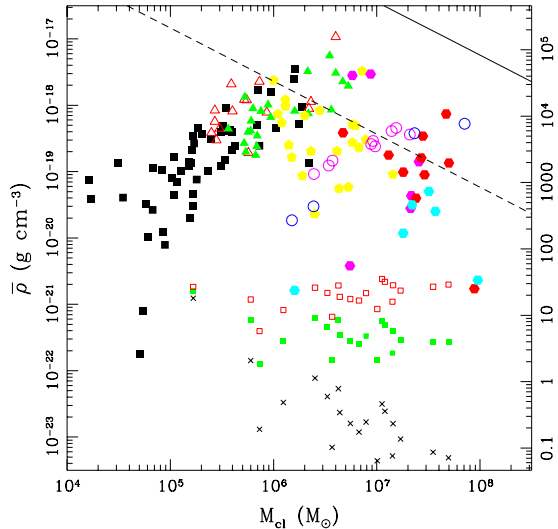


FIG. 7.— Mean cluster density  $\bar{\rho} = 3M_{cl}/(4\pi r_{cl}^3)$  as a function of cluster dynamical mass. The symbols are as in Fig. 6, with the following additions: Open triangles are M82 superstar clusters from McCrady & Graham (2007). Open magenta circles are nuclear star clusters from Walcher et al. (2005). Small crosses represent the mean density of Milky Way satellite dwarf galaxies evaluated at their core radii (typically substantially larger than 10 pc). The small filled (green) and open (red) squares represent the satellite galaxy densities extrapolated to 10 pc using either an NFW profile or a Moore et al. (1999) profile. The solid line at the upper right represents the initial density of radiation pressure supported star clusters (assuming 100% star formation efficiency, while the dashed line shows the radius after stellar evolution has reduced the mass to  $\alpha = 0.4$  of its initial values. The right hand vertical axis is labeled by the density in solar masses per cubic parsec. Note that the dark matter dominated dwarf galaxies have mean densities at 10 pc a factor of (at least) 30 less than the typical density of massive star clusters.

fact, numerical simulations find dark matter halos that follow a density profile given by Navarro et al. (1997)

$$\rho(r) = \frac{\rho_s}{(r/r_s)(1+r/r_s)^2}, \quad (32)$$

(the NFW profile) or the slightly steeper Moore et al. (1999) profile

$$\rho(r) = \frac{\rho_s}{(r/r_s)^{1.5}(1+(r/r_s)^{1.5})}. \quad (33)$$

If we assume  $r_s \gg r_c$  for the Milky Way dwarf satellites, we can scale the density to 10 pc; doing so, we find the small filled squares in Fig. 7 (NFW profile) and the small open squares (the Moore et al. (1999) profile). The maximum mean density at 10 pc is similar to that of Willman 1,  $\rho \approx 10^{-21} \text{ g cm}^{-3}$ , far too small to explain the high mass to light ratios of the massive star clusters and UCDs.

We show in appendix D that the relatively low inferred mean dark matter density at  $r = 10 \text{ pc}$  is consistent with the highest resolution simulations, e.g., Diemand et al. (2007).

We conclude that compact massive star clusters (GCs and UCDs) are not (non-baryonic) dark matter dominated. This does not mean that they contain no non-baryonic dark matter: if they form in the center of their own dark matter halo, the baryons will, when they collapse, gravitationally compress the inner part of the dark matter halo (Blumenthal et al. 1986). However, simple calculations show that the fraction of dark matter inside  $r_{cl}$  for objects as concentrated as the compact clusters is typically less than  $\sim 30\%$ .

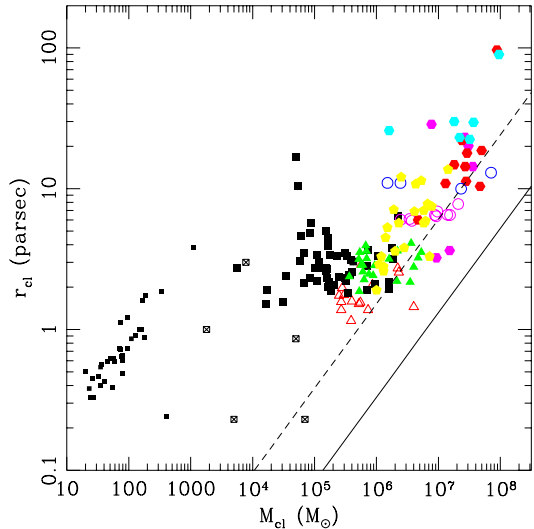


FIG. 8.— Cluster radius in parsecs plotted against cluster mass (in solar masses). Symbols are as in Fig. 7, with two additions: Small filled squares are embedded (young) Milky Way clusters from Lada & Lada (2003), while open squares with diagonals are massive young Milky Way clusters. The solid line shows the radiation radius computed from equation (17). The dashed line shows the cluster radius after mass loss (corresponding to a lockup fraction  $\alpha = 0.4$ ) assuming adiabatic expansion of the cluster.

#### 4.3. The mass-radius relation for massive clusters

We have already noted the striking observational result that both young moderately massive ( $10^4 M_{\odot} < M_{cl} < 10^6 M_{\odot}$ ) clusters and (old) globular clusters show no systematic variation of radius with mass. Equation (17) predicts that the mass of radiatively supported protoclusters should have radii that increase with increasing mass. We therefore expect that evolved massive clusters will inherit this mass-radius relation. Figure 8 shows the mass radius relation for low mass clusters in the Milky Way, and high mass clusters and ultra compact dwarfs (UCDs) from a variety of external galaxies. The prediction of equation (17) is shown as the solid line in the Figure. This is the initial radius of a cluster, before it has evolved, and should be compared with young massive clusters, such as those in M82 studied by McCrady et al. (2003) and McCrady & Graham (2007) (the open triangles in the Figure).

The dashed line is the predicted relation for old massive clusters; the initial  $M_{cl}$  has been reduced by the lockup fraction  $\alpha$  (taken to be fixed at 0.4, although it will vary with  $M_{cl}$ ), while  $r_{cl}$  has been increased by the same factor. This line should be compared to the old massive clusters and UCDs.

The fact that the low mass clusters ( $M_{cl} \lesssim 5 \times 10^5 M_{\odot}$ ) are well above the line indicates that something other than radiation supported these clusters when they formed, i.e., that radiation support was not important in their evolution. In contrast, the more massive clusters lie near the radius at which radiation support becomes important, and their radii do show a trend of increasing radius with increasing mass. This lends some credence to the notion that radiation plays a role in the formation of the most massive star clusters.

## 5. DISCUSSION

The properties of star clusters with masses ranging from  $\sim 100 M_{\odot}$  to  $10^8 M_{\odot}$  vary continuously with cluster mass, as

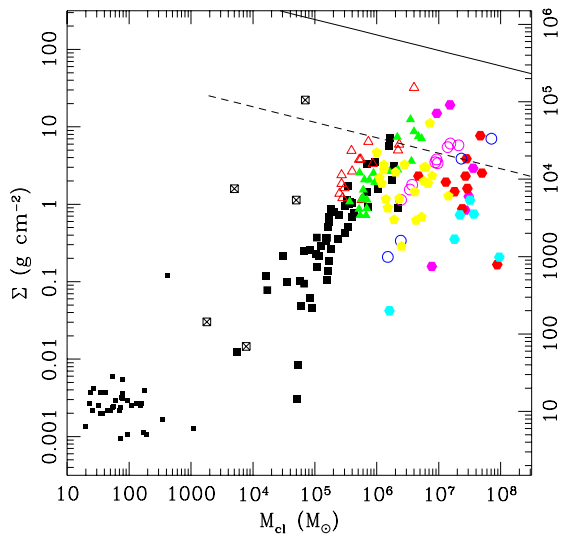


FIG. 9.— Cluster surface density plotted against cluster mass (in solar masses). Data points are as in Fig. 8. The solid line shows the maximum (initial) surface density allowed by the Eddington limit, equation (18). The dashed line shows the surface density after  $\sim 10$  Gyrs, with a lockup fraction  $\alpha = 0.4$ . The right hand vertical axis is labeled in units of solar masses per square parsec.

seen in Figures 6 through 9. There are sharp changes in the slope of cluster radius at  $M_{cl} \approx 10^4 M_{\odot}$  and at  $M_{cl} \approx 10^6 M_{\odot}$ , and associated features in  $\Sigma$ ,  $\rho$  and cluster escape velocity at these masses.

We have argued that the change of slope in  $r_{cl}(M_{cl})$  at  $M_{cl} = 10^6 M_{\odot}$  arises from the emergence of radiation pressure as a dynamically significant player in the formation of these massive clusters. The feature at  $M_{cl} = 10^4 M_{\odot}$  remains unexplained.

In contrast to the observation of two changes in the slope of  $r_{cl}$  with  $M_{cl}$ , there is a single change in the slope of  $\Upsilon_V$ , at  $M_{cl} \approx 10^6 M_{\odot}$ . We assert that this is due to the abrupt increase in gas temperature with increasing cluster mass, associated with the change from radiatively thin to radiatively thick cooling. The sharp jump in  $T(M_{cl})$ , the slower change of  $\rho(M_{cl})$ , and the stronger dependence of Jeans mass on  $T$  ( $M_J \sim T^{3/2}/\rho^{1/2}$ ) results in a rapid increase in Jeans mass with increasing cluster mass above  $M_{cl} = 10^6 M_{\odot}$ . We have identified this as the underlying cause for the increase in  $\Upsilon_V$  with increasing  $M_{cl}$  above  $\sim 10^6 M_{\odot}$ .

The results regarding the IMF found here (Figs. 2, 5, and the lines in Fig. 6) show that  $\Upsilon_V$  should increase with increasing cluster mass even in the absence of non-baryonic dark matter, up to values as large as 6, and possibly higher (the bulk of the extra mass is, in the case of a top heavy IMF, in the form of white dwarfs). We have also argued that non-baryonic dark matter in Galactic satellite galaxies on scales of  $\sim 10$  pc has densities smaller by a factor of 30 than the densities observed in massive star clusters and UCDs. It appears unlikely that the high mass to light ratios of the compact clusters are due to non-baryonic dark matter.

Fellhauer & Kroupa (2002) model UCDs as merged globular clusters. Their clusters, at  $M_{cl} = 2 \times 10^7 M_{\odot}$  and with radii ranging from 39 to 72 pc or larger, are larger than all but one of the objects plotted in Figure 8.

Bekki et al. (2001) and Bekki et al. (2003) argue that UCDs are the remnants of nucleated dwarf galaxies; the nuclei lose their envelopes due to tidal stripping in the gravitational field of their host cluster halos. This begs the question of how the nuclei formed. To address this question, Bekki et al. (2004) explore the same mechanism as Fellhauer & Kroupa (2002), merging of globular clusters. They find scaling relations that imply a mass radius relation

$$r_{cl} \sim M_{cl}^{0.38}, \quad (34)$$

which would imply, for example, that the surface density of massive clusters would increase with increasing mass. This would appear to be ruled out for clusters with  $M_{cl} \gtrsim 3 \times 10^6 M_{\odot}$ .

Globular clusters have mass to light ratios  $\Upsilon_V \approx 2$ , consistent with the notion that they contain no non-baryonic dark matter. Models for massive clusters that merge globulars will not naturally trap large masses of dark matter, so the merger products will also lack dark matter, and have  $\Upsilon_V \approx 2$ , smaller than the values observed for many of the UCDs shown in Figure 6.

Evstigneeva et al. (2007) find from spectroscopy that the ages, metallicities, and abundances of Virgo UCDs are similar to those of Virgo globular clusters. However, the mass to light ratios and the mass-radius relations differ. This is seen most clearly in the lower panel of their Figure 6, which is very roughly a plot of  $\Sigma$  against mass (as in Figure 9 here). They conclude that the internal properties of Virgo UCDs are consistent with them “being the high-mass/high-luminosity extreme of known GC populations”, apparently emphasizing the continuity of their distribution in the  $\kappa_2 - \kappa_1$  (roughly the  $\Sigma - M_{cl}$ ) fundamental plane rather than the clear break in the slope that they find.

In this work the break in scaling properties is attributed to the emergence of radiation pressure as a dynamically significant element in the formation of the cluster. This result strengthens the case for treating globular clusters and UCDs on a unified footing.

Mieske & Kroupa (2008) note the high values of  $\Upsilon_V$  found for UCDs, and suggest that it is due to a non-standard IMF. Their explanation is that the IMF is bottom-heavy, i.e., that there are more low mass stars per unit stellar mass than in the standard (Milky Way) IMF. It may appear paradoxical that high  $\Upsilon$  values arise from both top heavy and from bottom heavy IMFs, but in both cases one appeals to an excess of under-luminous stars. In a top heavy IMF, at late times, the extra dead weight is found in stellar remnants, while in bottom heavy IMFs, the dead weight is found in low mass stars (well below the main sequence turnoff). Mieske & Kroupa (2008) suggest observations of CO at  $2.3 \mu\text{m}$  as a way to test for the presence of large numbers of low mass stars.

Klessen et al. (2007) suggest that in warm star-bursting circumnuclear gas, as in the Galactic center, the IMF will be top heavy compared to the IMF rest of the Milky Way. They present numerical simulations showing that this is the case. They attribute the difference to the larger Jeans mass in the warm gas, as argued here. In this paper, we attribute the higher temperature to accretion of the cluster gas, as opposed to radiation from stars surrounding the proto-cluster; however, the crucial point is that higher temperatures in the ISM will lead to a top heavy IMF.

## 6. CONCLUSIONS

We have shown that the Jeans mass in a cluster is roughly independent of the cluster mass as long as the cluster is optically thin to the FIR, and assuming that the mass radius relation seen in embedded clusters reflects the primordial mass radius relation. Clusters forming today in the Milky Way are optically thin, so this finding is consistent with the observed constancy of the IMF in our galaxy.

Many Milky Way globular clusters were also optically thin, or had low enough velocities that their accretion luminosities would not have raised the gas temperature significantly. The Jeans mass in such clusters would then depend only on their radii at the time of formation.

However, we have pointed out that many clusters in other galaxies, and in the Milky Way in the past, are or were optically thick to the FIR; such clusters often (though not always) have high enough accretion luminosities that the gas temperature would have been higher than 10K. We went on to argue that the Jeans mass is larger than a solar mass in such clusters. Using the assumption that the break in the IMF is associated with the Jeans mass, we concluded that massive clusters should have high  $L/M$  ratios when young, and high  $M/L$  ratios when more than a few Gyrs old.

The prediction of high  $L/M$  is consistent with observations of apparently enhanced light to mass ratios in the superstar clusters M82-F and M82-11, although the optically thick clusters M82-9 and NGC 4038:W99-15 appear to have normal  $M/L$  ratios. Other superstar clusters in M82 and other nearby galaxies are optically thin, and so they should have normal IMFs. Clearly, more data on superstar clusters would be helpful.

A top heavy IMF, which we showed should occur in the most massive and compact globular clusters, will tend to produce an excess of LMXBs and pulsars in metal rich globular clusters in both the Milky Way and in nearby galaxies, and at

the same time, a higher  $M/L$  ratio.

Compelling support for the notion of a high mass to light ratio in massive clusters is supplied by Figure 6, which compares the predicted and observed mass to light ratio for objects with masses ranging up to  $10^8 M_\odot$ . As the solid lines in the Figure indicate, this result is consistent with the prediction of a top-heavy IMF resulting from the elevated temperatures associated with accretion in an optically thick environment.

We also argued that in the most massive clusters, with  $M_{cl} \gtrsim 3 \times 10^6 M_\odot$ , the substantial luminosity associated with the contraction of the cluster must have been dynamically important. The predicted mass-radius relation,  $r_{cl} \sim M_{cl}^{3/5}$ , leads to a number of relations between the properties of massive star clusters, involving the cluster velocity dispersion, the cluster luminosity, and the surface density; for example, we found  $L_V \sim \sigma^4$ . These relations appear to be consistent with the observed properties of massive star clusters.

The combination of strong evidence for a cluster-mass dependent mass to light ratio and for a mass-radius relation  $r_{cl} \sim M_{cl}^{3/5}$  provides solid support for the idea that a contraction powered radiation field has left its mark on the most massive star clusters we see around us.

It is fitting to close by emphasizing again the striking fact that globular clusters are observed to have radii of 2–3 parsecs, with only weak dependence on cluster mass over a range  $10^4 M_\odot$  to  $3 \times 10^6 M_\odot$ . The origin of this (lack of a) mass-radius relation remains a major puzzle.

The author is grateful to Natasha Ivanova for helpful discussions. This research has made use of the SIMBAD database, operated at CDS, Strasbourg, France, and of NASA's Astrophysics Data System. The author is supported in part by the Canada Research Chair program and by NSERC of Canada.

## APPENDIX

## LOG-NORMAL PROBABILITY DENSITY FUNCTIONS

Both analytic theory and numerical simulations of turbulent flows find that the density follows a log-normal probability density function. While the interpretation of observations is difficult, there are indications that gas in star forming regions in the Milky Way does as well. In this appendix we show that this fact implies that the characteristic density  $\rho_m$  of the gas out of which stars in star clusters form is no more than a factor of  $\sim 10$  larger than the mean density of the protocluster.

Following Ostriker Stone & Gammie (2001), let  $y = \log(\rho/\bar{\rho})$ , where the logarithm is base 10 and  $\bar{\rho}$  is the mean density of the cluster. Then the probability density function is

$$f_M(y) = \frac{1}{\sqrt{2\pi\sigma^2}} \exp[-(y-\mu)^2/(2\sigma^2)]. \quad (\text{A1})$$

The quantity  $f_M(y)dy$  is the fraction of the cluster mass with density contrast  $y$  in the interval  $(y, y+dy)$ . Demanding conservation of mass (in the form of the continuity equation) leads to a relation between the mean  $\mu$  and the dispersion  $\sigma$  of  $y$ :

$$\mu = \frac{1}{2} \ln(10)\sigma^2. \quad (\text{A2})$$

Letting

$$t = (y + \mu)/\sqrt{2}\sigma, \quad (\text{A3})$$

the fraction of the cluster mass having  $\rho > \rho_m$  is

$$f_g(> \rho_m) = \frac{1}{2} \text{erfc}(t_m). \quad (\text{A4})$$

Figure 10 plots both  $f_M(\rho/\bar{\rho})$  and  $f_g(> \rho_m)$ . We have taken  $\mu = 0.4$ ; in the simulations of Ostriker Stone & Gammie (2001) this corresponds to a fast magnetosonic Mach number  $M_F \approx 3$ .

If star formation occurs on a crossing time, the probability density function is sampled once before the protocluster gas is dissipated. During this time a fraction between 0.1 and 0.3 of the gas must form stars. These fractions are indicated by the upper two horizontal dotted lines in the Figure. The corresponding over densities are 5 and 14 times the mean density of the clump. Under the extreme assumption that only the densest gas in the protocluster forms stars, the Jeans mass of the relevant gas is factor between two and four smaller than the mean Jeans mass of the clump.

If star formation takes more than a single crossing time, the probability density is sampled more than once, so a larger fraction of the gas may be turbulently compressed to high density. The bottom dotted line corresponds to star formation in a cluster in which  $SFE = 0.1$  and for which star formation persisted for five dynamical times. We see that the characteristic density for this case is a factor 40 larger than the mean density, resulting in a Jeans mass 6.3 times smaller than the Jeans mass calculated using the mean density.

These estimates for the Jeans mass are likely underestimates; many self-gravitating bodies of gas with lower density but larger sizes will be produced by the turbulence, as argued by, e.g., Padoan & Nordlund (2002). In fact the argument made here is similar to that made by those authors; both rely on the steep decline in the PDF with increasing density. Here we are emphasizing the observational constraints provided by the SFE and estimates of the duration of star formation rather than the dynamical constraint that stars form out of self gravitating material.

#### LUMINOSITY FUNCTIONS AND INITIAL MASS FUNCTIONS

The number of stars in a cluster having a given mass is described by the initial mass function (IMF),  $\phi(m)dm$ , the number of stars with masses between  $m$  and  $m + dm$ , where  $m$  is measured in solar masses  $M_\odot = 2 \times 10^{33}$  g. The IMF is normalized so that

$$\int_{m_L}^{m_U} m\phi(m)dm = 1, \quad (\text{B1})$$

where  $m_L$  and  $m_U$  are lower and upper mass limits. We sometimes employ the Salpeter mass function, which for  $m_L = 0.1$ ,  $m_U = 100$ , is  $\phi_{Sal} = 0.17m^{-\alpha}$  with  $\alpha = 2.35$ . We also use the observed IMF for the Orion Nebula, given in Muench et al. (2002); for simplicity we set  $\phi(m) = 0$  for masses below  $0.025M_\odot$ .

$$\phi_{M,m_1}(m) \equiv \frac{dN}{dm} = N_0 \begin{cases} m^{-2.21} & m_U > m > m_1 \\ m_1^{1.15-2.21} m^{-1.15} & m_1 > m > m_2 \\ m_1^{1.15-2.21} m_2^{0.27-1.15} m^{-0.27} & m_2 > m > m_L \end{cases} \quad (\text{B2})$$

Muench et al. (2002) found  $m_1 = 0.6M_\odot$  and  $m_2 = 0.12M_\odot$ . The high mass end of the IMF is described by a power law with index  $\alpha = 2.21$ , similar to that of the Salpeter IMF. Note that we use  $dN/dm$  rather than  $dN/d \log m$ , so the exponents that appear here are equal to those quoted in (Muench et al. 2002) minus one, i.e., their exponent  $-1.21$  becomes our exponent  $-2.21$ , while their  $+0.73$  becomes  $-0.27$  here.

The Muench et al. IMF is similar to that of Kroupa (2001), which has a high mass slope of  $\alpha = 2.3$  and a low mass slope  $\alpha = 1.3$ , slightly steeper than that of Muench et al.

#### The light to mass ratio

We use the Padova stellar evolution tracks (Bertelli et al. (1994); Girardi et al. (1996); Girardi 2006, <http://pleiadi.pd.astro.it>) to find the luminosity of stars of mass  $m$  at an age of  $\approx 2.5$  Myrs. For stars with  $m < 9$  we use the isochrone for 4 Myrs; these stars contribute very little luminosity, so the error involved in doing so is minor. For more massive stars we searched the evolutionary tracks to find the age nearest 2.5 Myrs, since the luminosity of these stars varies rapidly with age. The result is  $L(m)$  in the form of a table.

To find the light to mass ratio for stars at an age of 2.5Myrs, we integrate

$$\int_{m_L}^{m_U} L(m)\phi(m)dm. \quad (\text{B3})$$

For a Salpeter IMF with  $m_L = 0.1$  and  $m_U = 120M_\odot$  (the estimated initial mass of  $\eta$  Carina) the light to mass ratio is 2010 in cgs units. Using the Muench et al. (2002) IMF with the  $m_L$  and  $m_U$ ,  $m_2 = 0.1$  and  $m_1 = 0.6$  the ratio is 4470. Part of this difference is due to the difference in slope at the high mass end of the two IMFs; using a slope of 2.21, the light to mass ratio of a simple powerlaw is 1790. The rest of the difference is due to what is effectively a low mass cutoff at  $m = 0.6$  for the Muench IMF. This factor of two difference in the light to mass ratio for the different IMFs will lead to a factor of two difference in the predicted efficiency of star formation.

In the main text we argue that  $m_1$  is set by the Jeans mass, and that the latter varies with cluster mass. Figure 3 shows the light to mass ratio for a Muench et al. IMF as a function of  $m_1$ , keeping  $m_L$ ,  $m_U$ , and  $m_2$  fixed at their original values.

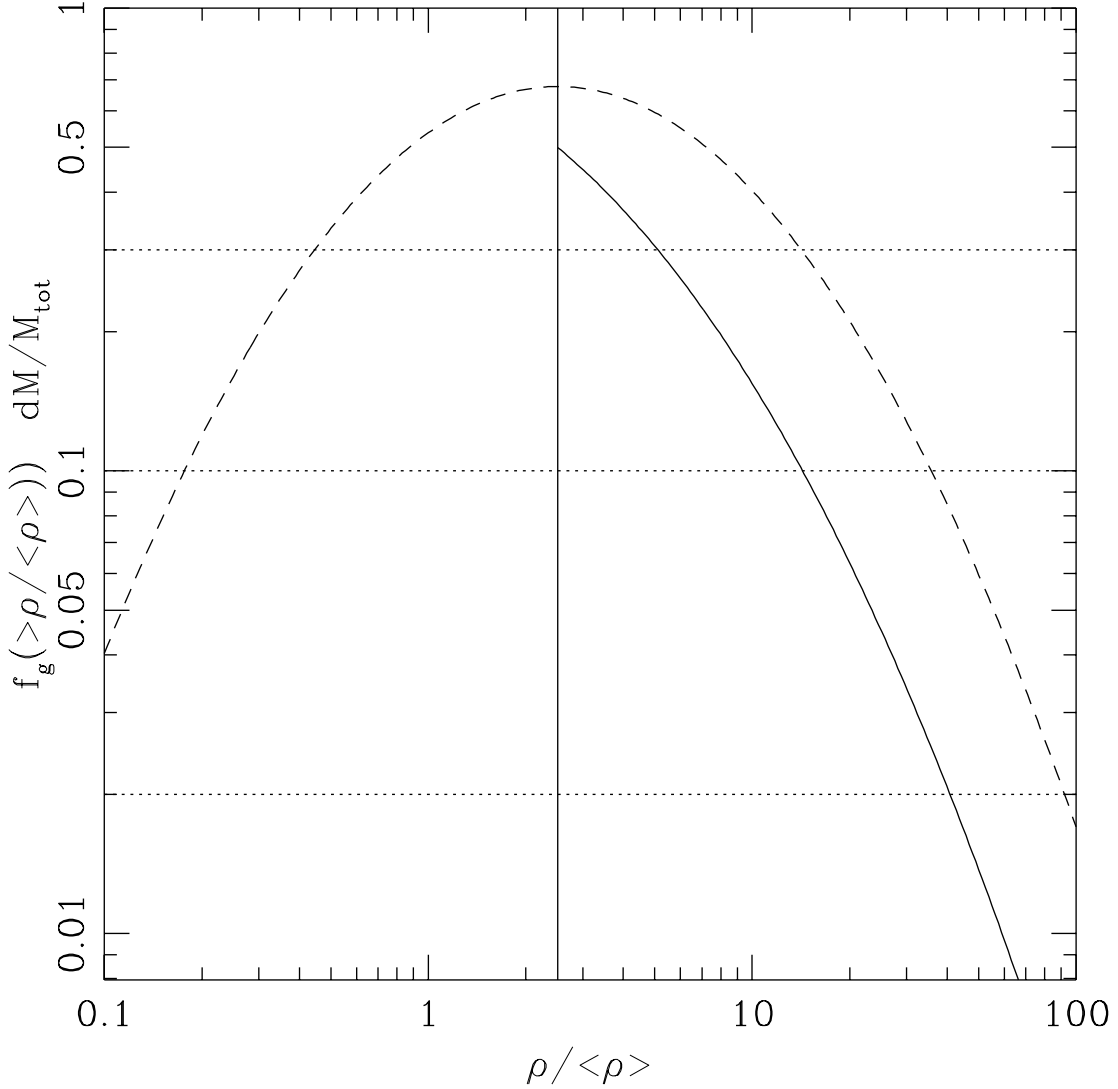


FIG. 10.— The solid line shows the gas fraction  $f_g(> \rho/\langle \rho \rangle)$  from eqn. A4. Also shown is the probability density function  $f_M(y) = dM/M_{tot}$  (dashed line) for  $\mu \equiv \langle \log \rho / \bar{\rho} \rangle_M = 0.4$  (corresponding to  $\mathcal{M}_F \approx 3$ ). The solid vertical line is at the mass-weighted mean density  $\mu$ . The horizontal dotted lines are drawn assuming that  $f_g = SFE$ , i.e., that only the densest gas in the cluster eventually ends up in stars, for  $SFE = 0.3, 0.1$ , and  $0.1/5$ . The value last assumes that the stars form over 5 dynamical times, so that  $f_M$  is sampled five times.

#### RADIATION PRESSURE SUPPORTED CLUSTER SIZES

While there is strong observational support for a characteristic globular cluster size, we are not aware of a good physical explanation for it, nor do we give one here. Instead, in this appendix we investigate the possibility that for massive clusters, the cluster length scale is determined by the interplay between the self-gravity of a clump of gas, the turbulent pressure  $\rho v_T^2$ , and in very dense and massive systems, radiation pressure. The turbulent pressure is

$$P_{turb} = \rho v_T^2. \quad (C1)$$

The turbulent velocity is well above the sound speed in the clusters under consideration here, so we expect that it will decay on the dynamical time of the cluster. The turbulent pressure therefor cannot halt the collapse of the protocluster, but should act to slow it. We assume that as the collapse proceeds, the gravitational binding energy released is converted into new turbulent motions, which then shock and dissipate their energy as heat. This heat is converted into thermal radiation, which then diffuses out of the cluster.

To model this, we assume that the turbulent pressure is a fixed fraction of the dynamical pressure, or, in terms of accelerations

$$a_{turb} = (1 - \gamma) |a_{grav}| = (1 - \gamma) \frac{GM(r)\rho}{r^2}. \quad (C2)$$

We usually take  $\gamma \approx 0.2$ ; choosing different values leads to different cluster radii and Jeans masses, when the protocluster is

radiatively supported.

The thermal radiation will diffuse out of the protocluster, but before it does it provides a pressure opposed to that of gravity:

$$P_{rad} = \frac{a}{3} T^4, \quad (C3)$$

where  $a = 4\sigma_B/c$  and  $\sigma_B$  is the Stefan-Boltzman constant. In the optically thick limit one can model this as a diffusion process, so that

$$P_{rad} = \frac{\kappa(T, \rho, Z)\rho L(r)}{4\pi r^2 c}, \quad (C4)$$

where  $\kappa(T, \rho, Z)$  is the Rossland mean opacity for the appropriate temperature, density, and metallicity. In our crude models we assume that the luminosity is roughly constant, independent of radius, as would be the case for a flow that is near free fall.

It is easy to show that for these massive clusters the gas pressure is negligible compared to the radiation pressure; one way to see this is note that the turbulent motions are highly supersonic.

The momentum equation for an infalling shell is

$$\frac{dv}{dt} = -\gamma \frac{GM(r)}{r^2} + \frac{\kappa L}{4\pi r^2 c}. \quad (C5)$$

The luminosity is given by

$$L = \frac{GMM}{r^2} v(t). \quad (C6)$$

Using this we can write

$$\frac{dv}{dt} = -\frac{GM(r)}{r^2} \left[ \gamma - \frac{\kappa M(r)}{c} \frac{v}{4\pi r^2} \right]. \quad (C7)$$

The first term on the right hand side of this equation is the effective (turbulence reduced) acceleration due to gravity, while the second term is the acceleration due to radiation pressure. The radiation term is proportional to the rate of collapse.

In our numerical work we start the integration at a large radius, where the second term is negligible. We stop the integration when the radiation pressure slows the collapse by 20–30% compared to the case with no radiation pressure. More exactly, if  $v_g \equiv \sqrt{GM_{cl}/r}$ , we define  $\tau_g \equiv r/v_g$  and  $\tau_{dyn} = r/v$ . We stop the calculation when  $\tau/\tau_g > 1.2$  or 1.3. Using the approximation that  $v \approx \sqrt{2\gamma GM(r)/r}$ , this occurs at a radius

$$r_{rad} = \phi_{rad} G^{1/5} \left( \frac{\kappa}{4\pi c} \right)^{2/5} M^{3/5}, \quad (C8)$$

where  $\phi_{rad}$  is a dimensionless constant; for our simple model,  $\phi_{rad} \approx 3$ .

The rationale for stopping the integration is that, when the dynamical time  $\tau_{dyn}$  exceeds the gravitational crossing time  $\tau_t$ , the cluster is partially supported by radiation pressure. The rate at which gravitational binding energy is converted into turbulent motion is reduced, so the level of turbulent pressure support will drop; the turbulent dissipation time will remain comparable to  $\tau_{grav}$ , so the turbulence will decay more rapidly than the cluster shrinks. We assume that as the turbulence decays, star formation will proceed at a rapid pace, and the cluster radius will be frozen in at or about the radius at which radiation pressure support becomes important.

#### NUMERICAL ESTIMATES OF DARK MATTER DENSITIES

In section §4.2.2 we argued by reference to the properties of known dark matter-dominated objects (Milky Way satellite dwarf galaxies) that dark matter densities on the scale of 10 pc were  $\rho_{DM} \sim 10^{-21} \text{ g cm}^{-3}$ , much less than the densities of massive compact star clusters ( $\rho \sim 10^{-19} \text{ g cm}^{-3}$ : see Fig. 7). In this appendix we use the results of numerical calculations to estimate the maximum density on small scales (Navarro et al. 1997; Bullock et al. 2001; Diemand et al. 2007; Madau et al. 2008).

It is traditional to use the concentration  $c_{vir} \equiv r_{vir}/r_s$ , where

$$r_{vir} \equiv \left( \frac{3M_{vir}}{4\pi \Delta_{vir} \rho_{crit}} \right)^{1/3} \quad (D1)$$

is the virial radius of a dark matter halo, and  $r_s$  is the characteristic radius of the density distribution, introduced in equations (32) and (33). In this expression  $\rho_{crit} \equiv 3H_0^2/(8\pi G) \approx 9 \times 10^{-30} \text{ g cm}^{-3}$  is the critical density of the universe and  $\Delta_{vir} \approx 200$ , depending on the cosmology, e.g.,  $\Delta_{vir} = 180$  for an Einstein-de Sitter cosmology.

We consider an NFW profile; results for Bullock et al. (2001) are similar. The mean density of an NFW halo at radius  $r$  is

$$\bar{\rho}(r) = 3\Delta_{vir}\rho_{crit} \left( \frac{r_{vir}}{r} \right)^3 \frac{A(r/r_s)}{A(c_{vir})}, \quad (D2)$$

where

$$A(x) = \ln(1+x) - \frac{x}{1+x}. \quad (\text{D3})$$

In the limit that  $r \ll r_s$  this is

$$\bar{\rho}(r) \approx 1500 \frac{c_{vir}^2}{A(c_{vir})} \left( \frac{M_{vir}}{10^8 M_\odot} \right)^{1/3} \left( \frac{10 \text{ pc}}{r} \right) \Delta_{vir} \rho_{crit}, \quad (\text{D4})$$

where we have scaled to the minimum virial mass for a cluster baryon mass of  $10^7 M_\odot$ . The value of  $c_{vir} \approx 10$  for a Milky Way size halo ( $M_{vir} \approx 10^{12} M_\odot$ ), leading to an estimate of  $\bar{\rho}(10 \text{ pc}) \approx 4 \times 10^{-21} \text{ g cm}^{-3}$ . From the results reported in Diemand et al. (2007) and Madau et al. (2008), the concentration  $c_{vir} \lesssim 50$  for  $M_{vir} \approx 10^8 M_\odot$  for subhalos near the center of their parent halo (note that both Fornax and Virgo UCDs are close to the centers of their parent halos). For these low mass compact halos, we find  $\bar{\rho}(10 \text{ pc}) \approx 3 \times 10^{-21} \text{ g cm}^{-3}$ , slightly higher than the observed densities of the Milky Way satellite galaxies (when extrapolated to  $r = 10 \text{ pc}$ ), but not nearly high enough to be dynamically important in the massive compact clusters and UCDs.

We note that the numerical calculations performed to date are not of high enough resolution to measure the density on scales of 10 pc. The highest resolution study published to date, that of Diemand et al. (2007), has a force resolution of  $\sim 90 \text{ pc}$ , sufficient to resolve clusters  $\sim 300 \text{ pc}$  in radius. Since we have no theoretical understanding of the density profiles found in the simulations, the extrapolation from 300 pc to 10 pc we use to estimate the dark matter densities is on shaky ground. For this reason we prefer the direct comparison with objects such as Willman I, where the dark matter density is measured directly on the relevant scale.

#### REFERENCES

- Adams, F. C., & Fatuzzo, M. 1996, *ApJ*, 464, 256  
 Allen, L., et al. 2007, *Protostars and Planets V*, 361  
 Barmby, P., McLaughlin, D. E., Harris, W. E., Harris, G. L. H., & Forbes, D. A. 2007, *AJ*, 133, 2764  
 Bastian, N., & Goodwin, S. P. 2006, *ArXiv Astrophysics e-prints*, arXiv:astro-ph/0604464  
 Bastian, N., Konstantopoulos, I., Smith, L. J., Tranco, G., Westmoquette, M. S., & Gallagher, J. S. 2007, *MNRAS*, 379, 1333  
 Bastian, N., Saglia, R. P., Goudfrooij, P., Kissler-Patig, M., Maraston, C., Schweize, F., & Zoccali, M. 2006, *A&A*, 448, 881  
 Baumgardt, H., & Kroupa, P. 2007, *MNRAS*, 380, 1589  
 Baumgardt, H., & Makino, J. 2003, *MNRAS*, 340, 227  
 Bekki, K., Couch, W. J., & Drinkwater, M. J. 2001, *ApJ*, 552, L105  
 Bekki, K., Couch, W. J., Drinkwater, M. J., & Shioya, Y. 2003, *MNRAS*, 344, 399  
 Bekki, K., Couch, W. J., Drinkwater, M. J., & Shioya, Y. 2004, *ApJ*, 610, L13  
 Bergin, E. A., & Tafalla, M. 2007, *ARA&A*, 45, 339  
 Bertelli, G., Bressan, A., Chiosi, C., Fagotto, F., & Nasi, E. 1994, *A&AS*, 106, 27  
 Blumenthal, G. R., Faber, S. M., Flores, R., & Primack, J. R. 1986, *ApJ*, 301, 27  
 Boily, C. M., Lançon, A., Deiters, S., & Heggie, D. C. 2005, *ApJ*, 620, L27  
 Bonnell, I. A., Bate, M. R., Clarke, C. J., & Pringle, J. E. 2001, *MNRAS*, 323, 785  
 Bonnell, I. A., Clarke, C. J., & Bate, M. R. 2006, *MNRAS*, 368, 1296  
 Bullock, J. S., Kolatt, T. S., Sigad, Y., Somerville, R. S., Kravtsov, A. V., Klypin, A. A., Primack, J. R., & Dekel, A. 2001, *MNRAS*, 321, 559  
 Clarke, C. J., Bonnell, I. A., & Hillenbrand, L. A. 2000, *Protostars and Planets IV*, 151  
 Clemens, D. P., & Barvainis, R. 1988, *ApJS*, 68, 257  
 Diemand, J., Kuhlen, M., & Madau, P. 2007, *ApJ*, 667, 859  
 Elmegreen, B. G. 2000, *ApJ*, 530, 277  
 Elmegreen, B. G., Klessen, R. S., & Wilson, C. D. 2008, *ArXiv Astrophysics e-prints*, arXiv:astro-ph/0803.4411  
 Evstigneeva, E. A., Gregg, M. D., Drinkwater, M. J., & Hilker, M. 2007, *AJ*, 133, 1722  
 Fall, S. M., Chandar, R., & Whitmore, B. C. 2005, *ApJ*, 631, L133  
 Fellhauer, M., & Kroupa, P. 2002, *MNRAS*, 330, 642  
 Fish, V. L., Reid, M. J., Argon, A. L., & Menten, K. M. 2003, *ApJ*, 596, 328  
 Freire, P. C., Kramer, M., Lyne, A. G., Camilo, F., Manchester, R. N., & D'Amico, N. 2001, *ApJ*, 557, L105  
 Geha, M., Guhathakurta, P., & van der Marel, R. P. 2002, *AJ*, 124, 3073  
 Girardi, L., Bressan, A., Chiosi, C., Bertelli, G., & Nasi, E. 1996, *A&AS*, 117, 113  
 Gomez, M., Hartmann, L., Kenyon, S. J., & Hewett, R. 1993, *AJ*, 105, 1927  
 Goodman, A. A., Pineda, J. E., & Schnee, S. L. 2008, *ArXiv Astrophysics e-prints*, arXiv:astro-ph/0806.3441  
 Gorjian, V., Turner, J. L., & Beck, S. C. 2001, *ApJ*, 554, L29  
 Gratton, R. G., Bragaglia, A., Carretta, E., Clementini, G., Desidera, S., Grundahl, F., & Lucatello, S. 2003, *A&A*, 408, 529  
 Harris, W. E. 1996, *AJ*, 112, 1487  
 Hasegan, M., et al., 2005, *ApJ*, 627, 203  
 Hillenbrand, L. A. 1997, *AJ*, 113, 1733  
 Hills, J. G. 1980, *ApJ*, 225, 986  
 Hilker, M., Baumgardt, H., Infante, L., Drinkwater, M., Evstigneeva, E., & Gregg, M. 2007, *A&A*, 463, 119  
 Jappsen, A.-K., Klessen, R. S., Larson, R. B., Li, Y., & Mac Low, M.-M. 2005, *A&A*, 435, 611  
 Jordan, A. 2004, *ApJ*, 613 L117  
 Kennicutt, R. C., Jr., Edgar, B. K., & Hodge, P. W. 1989, *ApJ*, 337, 761  
 Kharchenko, N. V., Piskunov, A. E., Röser, S., Schilbach, E., & Scholz, R.-D. 2005, *A&A*, 438, 1163  
 Klessen, R. S., Burkert, A., & Bate, M. R. 1998, *ApJ*, 501, L205  
 Klessen, R. S., Spaans, M., & Jappsen, A.-K. 2007, *MNRAS*, 374, L29  
 Kroupa, P. 1995, *MNRAS*, 277, 1491  
 Kroupa, P. 2001, *MNRAS*, 322, 231  
 Lada, E. A., & Lada, C. J. 1995, *AJ*, 109, 1682  
 Lada, C. J., & Lada, E. A. 2003, *ARA&A*, 41, 57  
 Larson, R. B. 1973, *Fundamentals of Cosmic Physics*, 1, 1  
 Larson, R. B. 2005, *MNRAS*, 359, 211  
 Leitherer, C., et al. 1999, *ApJS*, 123, 3  
 Li, Y., Klessen, R. S., & Mac Low, M.-M. 2003, *ApJ*, 592, 975  
 Low, C., & Lynden-Bell, D. 1976, *MNRAS*, 176, 367  
 Madau, P., Diemand, J., & Kuhlen, M. 2008, *ArXiv e-prints*, 802, arXiv:0802.2265  
 McCrady, N., Gilbert, A. M., & Graham, J. R. 2003, *ApJ*, 596, 240  
 McCrady, N., & Graham, J. R. 2007, *ApJ*, 663, 8  
 McKee, C. F., & Ostriker, E. C. 2007, *ARA&A*, 45, 565  
 McKee, C. F., & Williams, J. P. 1997, *ApJ*, 476, 144  
 Meurer, G. R., Heckman, T. M., Leitherer, C., Kinney, A., Robert, C., & Garnett, D. R. 1995, *AJ*, 110, 2665  
 Mieske, S., & Kroupa, P. 2008, *ApJ*, 677, 276  
 Miller, G. E., & Scalo, J. M. 1979, *ApJS*, 41, 513  
 Moore, B., Quinn, T., Governato, F., Stadel, J., & Lake, G. 1999, *MNRAS*, 310, 1147  
 Muench, A. A., Lada, E. A., Lada, C. J., & Alves, J. 2002, *ApJ*, 573, 366  
 Navarro, J. F., Frenk, C. S., & White, S. D. M. 1997, *ApJ*, 490, 493  
 Ostriker, E. C., Stone, J. M., & Gammie, C. F. 2001, *ApJ*, 546, 980  
 Padoan, P. 1995, *MNRAS*, 277, 377  
 Padoan, P., & Nordlund, Å. 2002, *ApJ*, 576, 870  
 Pagel, B. E. J. 1997, *Nucleosynthesis and Chemical Evolution of Galaxies*, by Bernard E. J. Pagel, pp. 392. ISBN 0521550610. Cambridge, UK: Cambridge University Press, October 1997.  
 Pryor, C., & Meylan, G. 1993, *Structure and Dynamics of Globular Clusters*, 50, 357  
 Rathborne, J. M., Jackson, J. M., & Simon, R. 2006, *ApJ*, 641, 389  
 Rees, M. J. 1976, *MNRAS*, 176, 483

- Rejkuba, M., Dubath, P., Minniti, D., & Meylan, G. 2007, *A&A*, 469, 147
- Richer, H. B., et al. 2004, *AJ*, 127, 2771
- Richer, H. B., et al. 2008, *AJ*, 135, 2141
- Roberts, M. S. 1988, *The Harlow-Shapley Symposium on Globular Cluster Systems in Galaxies*, 126, 411
- Robishaw, T., Quataert, E., & Heiles, C. 2008, *ApJ*, 680, 981
- Salpeter, E. E. 1955, *ApJ*, 121, 161
- Semenov, D., Henning, T., Helling, C., Ilgner, M., & Sedlmayr, E. 2003, *A&A*, 410, 611
- Smith, L. J., & Gallagher, J. S. 2001, *MNRAS*, 326, 1027
- Smith, L. J., Westmoquette, M. S., Gallagher, J. S., O'Connell, R. W., Rosario, D. J., & de Grijs, R. 2006, *MNRAS*, 370, 513
- Tan, J. C., Krumholz, M. R., & McKee, C. F. 2006, *ApJ*, 641, L121
- Thompson, T. A., Quataert, E., Waxman, E., Murray, N., & Martin, C. L. 2006, *ApJ*, 645, 186
- Turner, J. L., & Beck, S. C. 2004, *ApJ*, 602, L85
- Turner, J. L., Beck, S. C., Crosthwaite, L. P., Larkin, J. E., McLean, I. S., & Meier, D. S. 2003, *Nature*, 423, 621
- Vázquez, G. A., & Leitherer, C. 2005, *ApJ*, 621, 695
- Walcher, C. J., et al., 2005 *ApJ*, 618, 237
- Wong, T., et al., 2008 *MNRAS*, 386, 1069
- Zepf, S. E., Ashman, K. M., English, J., Freeman, K. C., & Sharples, R. M. 1999, *AJ*, 118, 752
- Zinnecker, H. 1982, *New York Academy Sciences Annals*, 395, 226